THE AMERICAN MINERALOGIST, VOL. 50, SEPTEMBER, 1965

SOME STABILITY RELATIONS IN THE SYSTEM $Mn\text{-}O_2\text{-}H_2O$ AT 25° AND ONE ATMOSPHERE TOTAL PRESSURE

OWEN BRICKER, *Harvard University, Cambridge, Massachusetts.*

ABSTRACT

Stability relations in the system $Mn\text{-}O_2\text{-}H_2O$ were investigated at 25° C. and one atmosphere total pressure. Seven compounds, $Mn(OH)_2$, Mn_3O_4, $\gamma\text{-}Mn_2O_3$, γ-MnOOH, $\delta\text{-}MnO_2$, $\gamma\text{-}MnO_2$, and hydrohausmannite were synthesized under controlled conditions of Eh and pH. Hydrohausmannite was found to be a mixture of Mn_3O_4 and/or $\gamma\text{-}Mn_2O_3$ and β-MnOOH rather than a single phase. The name feitknechtite is proposed for naturally occurring β-MnOOH. Free energy of formation data were obtained for the first six compounds listed. They are respectively: −147.14 kcal., −306.2 kcal., −132.2 kcal., −133.3 kcal., −108.3 kcal, and −109.1 kcal. Eh-pH diagrams were constructed to show stability relations among the phases in the system $Mn\text{-}O_2\text{-}H_2O$. Good correspondence was found between stability relations observed in the laboratory and those observed in natural occurrences of manganese oxides. A model is described for the supergene oxidation of rhodochrosite.

INTRODUCTION

Manganese, a transition metal, is capable of existing in a number of different oxidation states (2+, 3+, 4+, 6+, 7+). The 2+ and 4+ oxidation states are the lowest and highest that have been observed in nature, although the ephemeral existence of other states is conceivable. Commonly, manganese oxide minerals contain more than one oxidation state of manganese, and a continuous series between 2+ and 4+ is observed in the average oxidation state of manganese in supergene oxides (whether a 3+ oxidation state actually occurs in the solid state or is realized through an equal distribution of 2+ and 4+ states remains a moot question).

The mineralogy of the oxides, hydroxides and hydrous oxides of manganese is varied and complex. Application of *x*-ray diffraction techniques to the identification of these minerals has revealed a large group consisting of more than thirty mineral species (Hewett and Fleischer, 1960). A great many of these minerals are found in supergene deposits and have been formed by the supergene oxidation of manganese-rich protore. The assemblage of manganese oxide minerals in the system $Mn\text{-}O_2\text{-}H_2O$ observed in supergene deposits shows little variation with the type or origin of the protore from which it was derived. Commonly, the protore consists of rhodochrosite, either of sedimentary or hydrothermal origin, although silicate protore is not unknown. At a number of deposits the protore consists of carbonates containing as little as 2–3 per cent manganese (reported as $MnCO_3$).

The close similarity in oxide assemblage among the supergene deposits, regardless of protore type, indicates that the primary factors controlling the formation of this assemblage are the physico-chemical variables of the supergene environment; the temperature at a value close to the mean annual temperature of the region, the pressure at approximately one atmosphere. Under these conditions, each oxide mineral is stable only within certain limits of oxygen partial pressure, depending upon the oxidation state, or states, of manganese that it contains. The manganese oxides are sensitive to the intensity of the oxidizing conditions of their environment, and may be thought of as a sort of oxygen barometer that reflects the oxidation gradient in supergene processes. Because water is ubiquitous in the supergene environment, and Eh (oxidation potential) and pH (negative log of hydrogen ion activity) are easily measured variables in aqueous systems, it is convenient to express stability relations among supergene minerals in terms of these variables (Garrels, 1960).

Valuable information could be obtained concerning both the occurrence of manganese oxides and conditions pertaining in supergene deposits that contain manganese oxide minerals if thermochemical data were available for the manganese oxide species. Little data of this nature may be found in the literature, and the present study was undertaken to provide such data. The scope of the work is limited to the system Mn-O_2-H_2O at 25° and one atmosphere total pressure (Table 1).

Information derived from a study of this system provides data for a number of the important supergene oxides of manganese and serves as a point of departure for the investigation of those oxides containing additional components not included in this system.

EXPERIMENTAL PROCEDURE

The apparatus and procedures described below were used in most of the experimental work here reported. Where other apparatus or techniques were used a brief description of them is included.

The system under investigation was contained in a flat-bottom glass vessel of approximately 500 ml capacity. The rim of the vessel was ground plane and fitted with a plastic top through which a number of holes were drilled. This arrangement permitted electrodes, buret gas inlet tube, and thermometer to be inserted into the system, and aliquots of solution to be removed. When necessary, a gas-tight seal was effected by using stopcock grease between the plastic top and the ground-glass rim of the vessel. Temperature in the vessel was maintained at 25°±0.5° by enclosing it in a water jacket through which water from a constant temperature bath was circulated.

Eh was measured using a Beckman model WM millivolt-meter. The Eh electrode system consisted of a bright platinum electrode in conjunction with a saturated calomel reference electrode; a second platinum electrode was used for a solution ground. pH was measured using a Beckman model W pH meter. The electrode system consisted of glass electrode (Beckman 8990-80) in conjunction with a saturated calomel reference electrode, a platinum solution ground, and a thermal compensator. Eh and pH were recorded continuously for the duration of the run on a model Y153×89-C-11-111-26 Minneapolis-Honeywell recorder.

The oxidation potential of the system was regulated in various ways. In runs made at very low oxidation potentials hydrogen gas was initially used to reduce the system. Nitrogen gas, purified of CO_2 and O_2 by passing it through ascarite and then through a V^{3+} solution, provided an inert atmosphere and prevented diffusion of atmospheric oxygen and carbon dioxide into the system.

Either air, purged of CO_2 by passing it through ascarite, or oxygen gas was used to provide an oxidizing atmosphere. Oxidation was also achieved in some runs by using hydrogen peroxide. The highest oxidation potentials observed in these experiments were reached through disproportionation of manganese compounds such as Mn_3O_4 into Mn^{2+} and one of the non-stoichiometric forms of MnO_2. These reactions will be discussed in more detail in a subsequent section.

TABLE 1. MANGANESE COMPOUNDS IN THE SYSTEM Mn-O_2-H_2O AT 25° C. AND ONE ATMOSPHERE TOTAL PRESSURE

Compound	Mineral Name	Composition
MnO	Manganosite	MnO
$Mn(OH)_2$	Pyrochroite	$Mn(OH)_2$
Mn_3O_4	Hausmannite	Mn_3O_4
γ-Mn_2O_3[1]	———	$MnOOH$
α-$MnOOH$	Groutite	$MnOOH$
β-$MnOOH$	Feitknechtite[2]	$MnOOH$
γ-$MnOOH$	Manganite	$MnOOH$
Mn_2O_3	Bixbyite	Mn_2O_3
δ-MnO_2	Birnessite[3]	$(Na, Ca)Mn_7O_{14}2\cdot 8H_2O$
γ-MnO_2	Nsutite	$Mn_{1-x}Mn_xO_{2-2x}(OH)_{2x}$
β-MnO_2	Pyrolusite	MnO_2
MnO_2	Ramsdellite	MnO_2

[1] The terminology of Verwey and DeBoer (1936) was retained for this compound although in this study it was found to contain one water of hydration rather than being anhydrous. No natural occurrences of this compound have been described.

[2] Described in this study. The mineral hydrohausmannite was found to be a mixture of Mn_3O_4 and β-$MnOOH$ rather than a single phase.

[3] Formula given by Jones and Milne (1956) calculated from analysis of an impure sample. δ-MnO_2, a compound containing only manganese, but giving an x-ray pattern identical to birnessite has been prepared by a number of different investigators.

All chemicals used in the experimental work were of reagent grade. Distilled water, purged of CO_2 and O_2, was used in the preparation of all solutions. Before any reactions were initiated in the reaction vessel described above, the system was purged of oxygen and CO_2 with pure nitrogen gas.

The pH electrode system was standardized against two buffer solutions before each run. In most cases pH7 and pH4 buffers were used. pH9 buffer was also used occasionally. Standardization procedures always provided buffer checks within ±0.02 pH units of the pH value of the buffer solution. This is within the limit of error specified by the manufacturer of these buffers. The pH electrode system was also checked after each run. In a normal run lasting several days, no discernible drift occurred in the electrode standardization.

The Eh electrode system was periodically checked against Zobell's solution (Zobell, 1946). The potential reading observed was always within several millivolts of the potential specified for Zobell's solution.

The system was stirred constantly to prevent inhomogeneity. A magnetic stirrer was placed beneath the reaction vessel and a teflon-coated stirring bar placed in the vessel. This arrangement provided a vigorous stirring action.

Aliquots of solution were periodically removed from the vessel and filtered through a 0.22μ millipore filter. The oxidation products were identified by *x*-ray diffraction. In most runs only small quantities of solid were produced, and therefore it was necessary to use a powder camera rather than the faster diffractometer method. For routine identification a Straumanis type 57.3 mm diameter powder camera was employed. Reported d spacings were measured on films taken with a Straumanis type 114.6 mm diameter camera. A Philips *x*-ray diffraction unit employing Mn filtered iron ($K_\alpha = 1.9373$ Å) radiation was used for all *x*-ray work here reported.

EXPERIMENTAL DETERMINATION OF THE STABILITIES OF PHASES IN THE SYSTEM $Mn\text{-}O_2\text{-}H_2O$ AT 25°C. AND ONE ATMOSPHERE TOTAL PRESSURE

Pyrochroite, $Mn(OH)_2$

The mineral pyrochroite, first described by Igelström (1864) has a layer structure of the brucite type, space group $C\bar{3}m$ with $a=3.35$ and $c=4.69$ Å (Aminoff, 1919). Watanabe *et al.* (1960) obtained unit cell dimensions of $a=3.323$ $c=4.738$ Å for pyrochroite from the Noda-Tamagawa Mine, Japan.

1. *Preparation*

De Schulten (1887) prepared $Mn(OH)_2$ by treating a manganous chloride solution with concentrated alkali hydroxide under a hydrogen atmosphere. He obtained crystals up to 0.2 mm in diameter by redissolving the precipitate in its mother liquor at elevated tempertaure and cooling slowly. Simon and Fröhich (1937) and Moore, Ellis and Selwood (1950) used De Schulten's procedure to prepare $Mn(OH)_2$. Klingsberg (1958) prepared $Mn(OH)_2$ by subjecting manganese metal to 200 psi of water pressure at 363° C. for one day. He found that the transition $MnO \rightleftharpoons Mn(OH)_2$ could be made to proceed reversibly at elevated temperature by varying the water pressure, and has determined the P_{H_2O} (psi)—T° C. curve for the reaction.

In this study $Mn(OH)_2$ was precipitated from dilute manganous nitrate, perchlorate, and sulfate solutions at 25° C. and one atmosphere total pressure in an oxygen-free environment by increasing the pH with dilute sodium hydroxide. No attempt was made other than aging the precipitate in the solution, to increase its crystallinity. It was found that the same quality *x*-ray diffraction patterns were obtained regardless of whether the fresh precipitate was *x*-rayed immediately or aged for several days in the solution. The reflections on these patterns are strong and sharp, indicating that the fresh precipitate is well crystallized. Feitknecht and Marti (1945) obtained similar results in their investigations of the aging of $Mn(OH)_2$. *X*-ray data for pyrochroite and for $Mn(OH)_2$ prepared in this study are compared in Table 2.

TABLE 2. *X*-RAY DATA FOR PYROCHROITE AND $Mn(OH)_2$

Pyrochroite Nordmark, Sweden (Ramdohr, 1956)		Pyrochroite Noda-Tamagawa Mine Iwate, Japan (Watanabe *et al.*, 1960)		$Mn(OH)_2$ (Klingsberg, 1958)		$Mn(OH)_2$ (This study)	
d	I	d	I	d	I	d	I
4.91	w						
4.65	vs	4.743	100	4.728	100	4.72	9
4.52	vw						
2.85	m	2.897	10	2.870	14	2.87	4
2.43	s	2.460	40	2.453	40	2.45	10
2.36	vw			2.361	6	2.36	<1
1.81	s	1.829	20	1.825	26	1.826	6
1.65	m	1.661	10	1.658	6	1.658	4
1.56	m	1.568	5	1.567	4	1.565	3
						1.434	<1
1.38	m	1.384	5	1.381	8	1.382	2
						1.374	2
				1.346	2	1.356	<1
1.22	m	1.230	5 Broad			1.227	2
1.18	w			1.180	3	1.182	<1
1.14	vw					1.143	1
1.09	w					1.095	<1
						1.085	1
1.06	m					1.062	2
.984	w					.987	2

No chemical analysis of $Mn(OH)_2$ was made owing to the difficulty in preventing oxidation during handling. Aliquots of the $Mn(OH)_2$ suspension treated with o-tolidine and examined spectrophotometrically showed no signs of the presence of oxidation states higher than Mn^{2+}.

Bäckströmite, an orthorhombic modification of $Mn(OH)_2$ from Långban, Sweden, has been reported by Aminoff (1919). Buerger (1937) has suggested that bäckströmite is actually pyrochroite pseudomorphous after manganite. Grigoriev (1934) claimed to have prepared this modification at temperatures above 80° C in the presence of a large excess of water. No evidence for an orthorhombic modification of $Mn(OH)_2$ was found in this study.

2. *The equilibrium constant and free energy of* $Mn(OH)_2$

The equilibrium constant of $Mn(OH)_2$ has been determined by a number of investigators (Table 3). Because of the diversity of values obtained in these investigations, the equilibrium constant was redetermined.

Three sets of experiments were made. In the first two sets, manganese sulfate solutions of known concentration were titrated with NaOH until approximately half of the Mn^{2+} was precipitated as $Mn(OH)_2$ (the amount precipitated being known exactly). The pH was measured, then known amounts of KCl or KNO_3 solution were added to increase ionic strength, and the pH recorded after each addition. In the last set of experiments, the ionic strength was moderated by adjusting the concentration of manganese sulfate rather than adding neutral salts. A nitrogen atmosphere was used in all of the experiments to prevent oxidation. The concentration of Mn^{2+} remaining in solution is known from the stoichiometry of the reaction, pH is a measure of a_{H^+}, and $K_w = a_{H^+} X\ a_{OH^-}$; therefore

TABLE 3. EQUILIBRIUM CONSTANT AND FREE ENERGY OF FORMATION OF $Mn(OH)_2$

Investigator	Log K	$F°_{Mn(OH)_2}$[1]
Herz (1900)	−12.1	−146.0 kcal.
Sackur and Firtzmann (1909)	−13.4	−147.8 kcal.
Britton (1925)	−13.89	−148.49 kcal.
Oka (1938)	−12.9	−147.1 kcal.
Fox, *et al.*, (1941)	−12.8	−146.9 kcal.
Nasanen (1942)	−12.72	−146.89 kcal.
Kovalenko (1956)	−12.35	−146.39 kcal.
This work (1963)	-13.01 ± 0.04	-147.34 ± 0.05 kcal.

[1] Calculated from the reported K values using the free energy values for $Mn_{aq}{}^{2+}$ and $OH_{aq}{}^{-}$ listed by Latimer (1952).

$$a_{OH^-} = \frac{K_W}{a_{H^+}} \tag{1}$$

where a_{OH^-} and a_{H^+} are the activities of hydrogen ion and hydroxyl ion and K_w is the dissociation constant of water. The concentrations of Na^+ and $SO_4{}^{2-}$ in the system are also known, as are the concentrations of neutral salts added to the system. Using this data, a mixed activity-concentration constant K^1, can be calculated for $Mn(OH)_2$:

$$K^1 = a^2_{OH^-}C_{Mn^{2+}} \tag{2}$$

where $C_{Mn^{2+}}$ is the concentration of manganous ion remaining in solution.

The activity of an ion is related to its concentration by:

$$C_i = \frac{a_i}{\gamma_i} \tag{3}$$

where γ_i is the activity coefficient of i, and equation (2) can be rewritten:

$$K^1 = a^2_{OH^-} \cdot \frac{a_{Mn^{2+}}}{\gamma_{Mn^{2+}}} \tag{4}$$

The thermodynamic stability constant, K, for $Mn(OH)_2$ is given by:

$$K = a_{Mn^{2+}}a^2_{OH^-} \tag{5}$$

Therefore K is related to K^1 by:

$$K = K\gamma_{Mn^{2+}} \tag{6}$$

Log K^1 values were plotted against the square root of ionic strength and the curve extrapolated to zero ionic strength (Fig. 1, 2, 3).[1] The ionic strength is given by:

$$I = 1/2\sum C_iZ_i^2 \tag{7}$$

where C_i is the molal concentration of species i, and Z_i its charge. At zero ionic strength $\gamma Mn^{2+} = 1$ and $K^1 = K$.

The Debye-Hückel theory can be used to determine the limiting slope in this extrapolation.

From the Debye-Hückel theory:

$$-\log \gamma_{Mn^{2+}} = \frac{4A\sqrt{I}}{1 + \mathring{a}B\sqrt{I}} \tag{8}$$

where A and B are constants, the values of which depend upon the nature of the solvent, the temperature and the pressure, and å is the effective diameter of the ion in solution. Rewriting equation (6) in logarithmic form and substituting for Mn^{2+}.

$$\log K = \log K^1 - \frac{4A\sqrt{I}}{1 + \mathring{a}B\sqrt{I}} \tag{9}$$

---

[1] Tables listing results of all equilibration runs have been deposited as document No. 8509 with the American Documentation Institute, Auxiliary Publications Project, Photoduplication Service, Library of Congress, Washington 25, D.C. Copies may be secured by citing the document number, and remitting $2.50 for photoprints or $1.75 for 35 mm microfilm. Advance payment is required.

In dilute solutions at 25° C. the term $1+\text{å}B\sqrt{I}$ approaches unity, the constant A is approximately 0.5, and the equation reduces to:

$$\log K = \log K^1 - 2\sqrt{I} \tag{10}$$

Log K^1 is a linear function of the square root of ionic strength. The limiting slope is -2.

In Fig. 1, 2, and 3 both log K^1 and log K values have been plotted against the square root of ionic strength. The log K values were determined by multiplying log K^1 values by the activity coefficient, $\gamma_{Mn^{2+}}$, calculated from the Debye-Hückel equation. In the experiment using sulfate ion to moderate ionic strength, the log K values were first calculated neglecting the weak $MnSO_4°$ complex (Bjerrum *et al.*, 1958). These log K values all fall below -13.01, the extrapolated value from the other experimental data. Recalculation of log K, taking into account the $MnSO_4°$ complex, yields values in line with the chloride and nitrate experiments. The $MnOH^+$ complex (Perrin 1962) was not found to be important over the concentration range of Mn^{2+} used in these experiments. The log K values are constant within the limits of error involved in measurement of pH and Mn^{2+} concentration with the exception of a few values. The log K^1 curves were extrapolated to zero ionic strength along

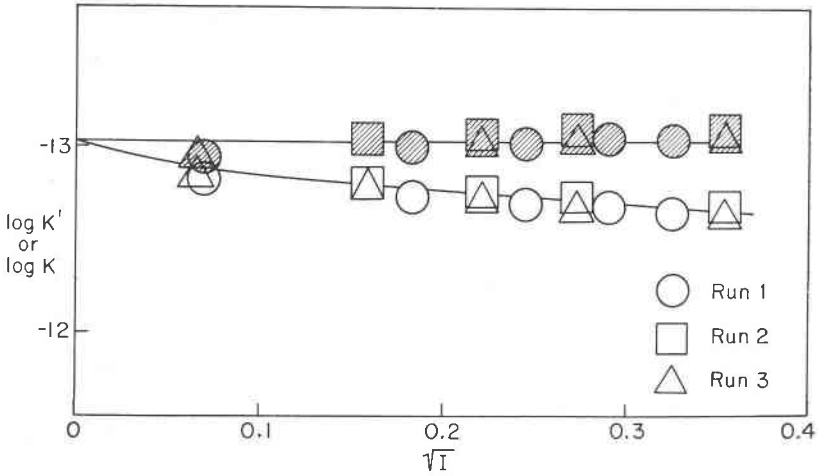

FIG. 1. Activity product of $Mn(OH)_2$ determined by extrapolating log K^1 values to infinite dilution using the Debye-Hückel limiting slope. Ruled figures are log K values calculated from the experimental data using the Debye-Hückel equation to obtain $\gamma_{Mn^{2+}}$. Ionic strength moderated by KCl. Size of circles indicates precision of measurement.

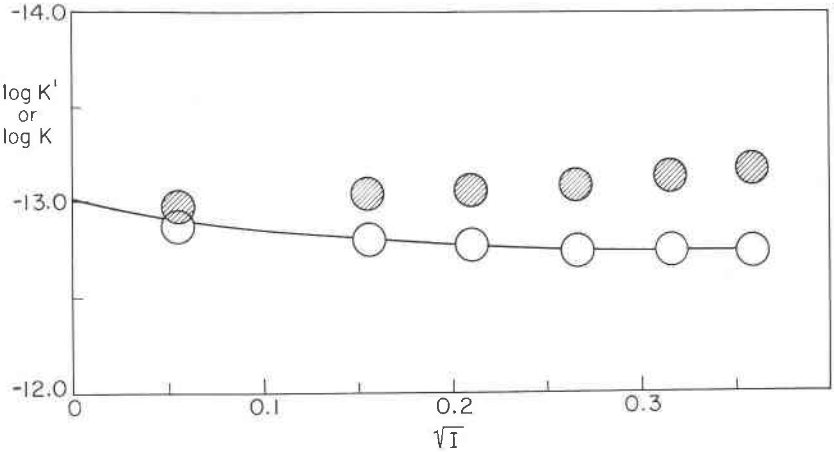

FIG. 2. Same as 1 but ionic strength moderated by KNO_3.

the limiting slope of −2 in the regions of the square root of ionic strength <05.

The Debye-Hückel limiting law describes the behavior of activity coefficients with very good accuracy in this concentration range (Robinson and Stokes, 1959, pp. 230–231). Extrapolation of the curves to zero ionic strength leads to a value of -13.01 ± 00.4 for log $K_{Mn(OH)_2}$, slightly smaller than the results of Oka (1938). The free energy of formation of $Mn(OH)_2$ calculated using the log K value reported above, and the free energy values of Mn_{aq}^{2+} listed by Latimer (1952) is $-147.34 \pm .05$ Kcal.

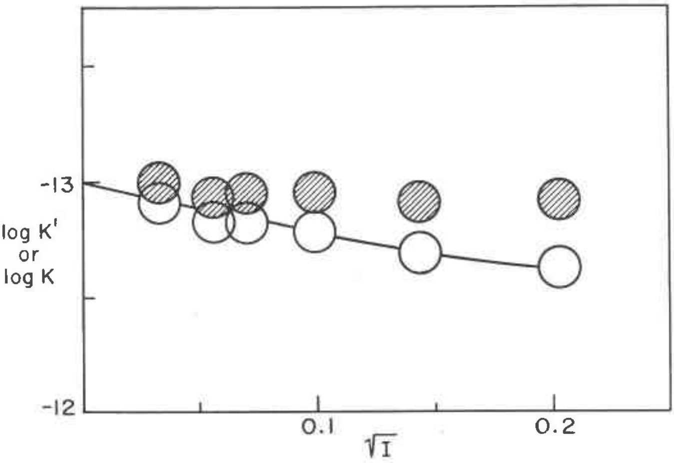

FIG. 3. Same as 1 but ionic strength moderated by $MnSO_4$.

This is 0.4 Kcal more negative than the value which Latimer calculated from the work of Fox, Swinehart and Garret (1941).

Hausmannite, Mn_3O_4

Naturally occurring Mn_3O_4 was first noted by Werner in 1789. Haidinger (1827) named this material hausmannite. Hausmannite has a tetragonally distorted spinel structure,[1] space group *I4/amd,* with $a=5.76$ and $c=9.44$ Å (Aminoff, 1936). The unit cell contains $Mn_4Mn_8O_{16}$.

1. *Preparation*

Mn_3O_4 can quite easily be prepared in pure form by any one of a number of methods. Most preparation procedures utilize high temperature in the presence of air to effect the decomposition of manganous salts and subsequent oxidation to Mn_3O_4, or, alternatively, the decomposition and reduction of Mn_2O_3 or MnO_2 to Mn_3O_4.

Shomate (1943) obtained high purity Mn_3O_4 by decomposition of electrolytic MnO_2 at 1050° C. Millar (1928), Southard and Moore (1942), and Moore, Ellis and Selwood (1950) prepared Mn_3O_4 by the thermal decomposition of manganous sulfate in air at about 1000° C. Klingsberg (1958) prepared Mn_3O_4 by hydrothermal techniques. Krull (1932) reduced MnO_2 to Mn_3O_4 with hydrogen gas at 200° C. Mn_3O_4 can be prepared from any of the oxides, hydrous oxides or hydroxides of manganese, as well as from a variety of manganous salts (e.g. chloride, nitrate, sulfate) merely by thermal decomposition in air at about 1000° C. Mn_3O_4 can also be prepared by oxidation of an aqueous suspension of manganous hydroxide (Feitknecht and Marti, 1945).

In this study it was found that Mn_3O_4 could be prepared and preserved indefinitely in an aqueous environment under controlled conditions of Eh and pH. Electron micrographs showed that the product consisted of well formed crystals of pseudocubic habit (Fig. 4). Mn_3O_4 was prepared from solutions of manganous nitrate, sulfate and perchlorate. First $Mn(OH)_2$ was precipitated by alkalization of the manganous solution with sodium hydroxide; then the $Mn(OH)_2$ suspension was oxidized with air purged of CO_2 or with oxygen gas. Slow oxidation of the $Mn(OH)_2$ suspension led to the formation of a cinnamon-brown compound which had an *x*-ray pattern identical to that of hausmannite (Table 4). Chemical analysis of this material from three separate preparations yielded calculated formulas of $MnO_{1.328}$, $MnO_{1.338}$ and $MnO_{1.338}$ with an error of ± 0.01 (analyzed by the method of Gattow, 1961). Water content was determined on only the first of these samples after drying to

---

[1] At temperatures above 1170° C. hausmannite inverts to a cubic structure (McMurdie *et al.*, 1950).

constant weight at 110° C. 1.37 per cent water was found. It is difficult to assess the role of water in very fine precipitates. There are examples of finely divided materials which tenaciously hold traces of non-essential water to temperatures of 500–600° C. Whether or not the water found in the Mn_3O_4 preparation is essential or merely adsorbed or included water cannot be determined with certainty.

2. *Free Energy of Formation of* Mn_3O_4

Maier (1936) calculated a value of −319.82 kcal as the free energy of formation of Mn_3O_4, using Roth's (1929) value of heat of formation and a calculated entropy. Shomate (1943) reviewed the heat of formation data for Mn_3O_4, all of which had been determined by combustion methods, and redetermined these data using heat of solution methods. Rossini *et al.* (1950) list a value of −306.0 kcal as the free energy of formation of Mn_3O_4. Mah (1960), using Shomate's heat of solution data and a correction factor given by Brewer (1953) calculated a value of −305.85 kcal as the free energy of formation of Mn_3O_4.

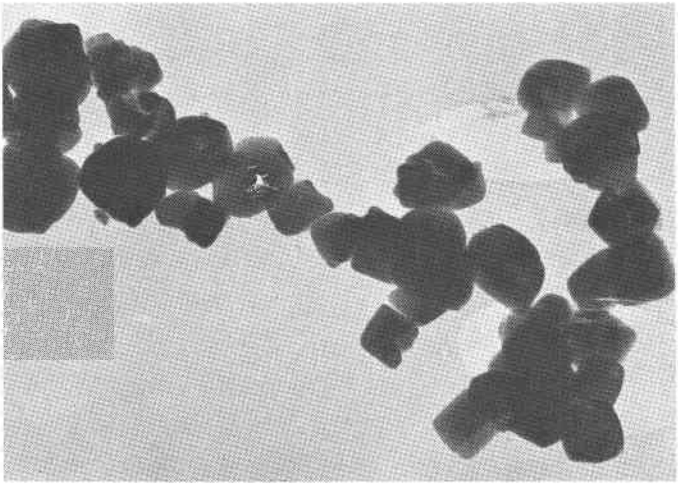

FIG. 4. Electron micrograph of Mn_3O_4 showing crystals of pseudocubic habit. ×80,000.

In this study Mn_3O_4 was prepared in an aqueous environment by the method described above, and the Eh and pH of the suspension was recorded during the oxidation reaction. Provided the Nernst relation is obeyed, the potential of the system is a function of pH and of the Mn^{2+} activity. For the reaction:

$$3\,Mn^{2+} + 4\,H_2O = Mn_3O_4 + 8\,H^+ + 2e^- \qquad (11)$$

TABLE 4. *X*-RAY DATA FOR HAUSMANNITE, Mn_3O_4, AND γ-Mn_2O_3

Hausmannite Ilfeld, Harz Germany (Ramdohr, 1956)		Mn_3O_4 (Moore *et al.*, 1950)		Mn_3O_4 (This work)		γ-Mn_2O_3 (This work)	
d	I	d	I	d	I	d	I
4.92	m	4.90	.21	4.92	8	4.92	7
3.08	s	3.08	.42	3.08	8	3.08	9
2.87	vw	2.87	.16	2.87	2	2.88	2
2.75	s	2.76	.60	2.76	9	2.76	9
2.48	vs	2.48	1.00	2.48	10	2.49	10
2.36	m	2.36	.25	2.36	4	2.36	3
2.03	m	2.03	.21	2.03	6	2.04	6
1.82	vw			1.828	5	1.83	1
1.79	m	1.80	.34	1.795	4	1.79	3
1.70	vw			1.700	2	1.70	2
1.64	vw			1.641	2	1.64	1
1.57	s	1.58	.32	1.575	4	1.57	3
1.54	vs	1.55	.63	1.542	9	1.54	8
1.44	s	1.44	.26	1.440	3	1.44	3
1.38	vw			1.381	1	1.38	1
1.34	vw			1.346	2	1.34	3
1.28	m	1.28	.14	1.277	3	1.28	2
1.23	w			1.229	2	1.23	1
1.19	vw			1.193	2	1.19	1
1.18	vw			1.180	2	1.18	1
1.12	m			1.122	1	1.12	1
1.10	vw			1.099	1	1.10	1
1.08	m			1.081	2	1.08	1
1.06	vw			1.061	1	1.06	1
1.03	m			1.030	2		
1.02	m			1.019	2	1.02	2
.985	m			.985	2		

the potential is:

$$\mathrm{Eh} = \mathrm{E}^\circ - 0.236\,\mathrm{pH} - 0.0891 \log a_{\mathrm{Mn}^{2+}} \qquad (12)$$

The experimental design permits Eh and pH to be measured, concentration of Mn^{2+} is known and can be converted to activity by application of the Debye-Hückel equation. Therefore, the standard potential of the reaction, E°, can be calculated.

$$\mathrm{E}^\circ = \mathrm{Eh} + 0.236\,\mathrm{pH} + 0.0891 \log a_{\mathrm{Mn}^{2+}} \qquad (13)$$

From the standard potential, the free energy of the reaction can be calculated.

$$\Delta \mathrm{F}^\circ_{\mathrm{R}} = n\mathrm{E}^\circ \mathfrak{F} \qquad (14)$$

where n is the number of electrons involved in the reaction and $\mathfrak{F}$ is the faraday constant. If the free energies of all other species involved in the reaction are known, the free energy of Mn_3O_4 can be calculated.

$$\Delta F^{\circ}_{Mn_3O_4} = \Delta F^{\circ}_{R} + 3\,\Delta F^{\circ}_{Mn^{2+}} + 4\,\Delta F^{\circ}_{H_2O} \tag{15}$$

The Eh-pH curves of two oxidation experiments are shown in Figs. 5 and 7. Figures 6 and 8 are the corresponding plots of E° as a function of the reciprocal of the square root of time. The theoretical slope for reaction (11) is -0.236 pH. The E° curves are constant within the limits of error of measurement of Eh and pH, the E° values being 1.809 v. and 1.825 v. for runs one and two respectively. Free energy values for Mn_3O_4 calculated from these E° values and the free energies of $Mn_{aq}{}^{2+}$ and H_2Oaq listed by Latimer (1952) are -306.5 kcal. and -305.8 kcal. These free energy values are in reasonable agreement with the free energy values listed by Latimer and Mah which were calculated from calorimetric data.

In a separate set of experiments Mn_3O_4 was prepared by thermal decomposition of $MnSO_4 \cdot H_2O$ at 1000° C. This Mn_3O_4 was then placed in a slightly acid environment (pH 5) and Eh and pH recorded. Mn^{2+} concentration was determined colorimetrically. The E° values were reproducible to ± 0.01 v. and corresponded to the values obtained above.

$\gamma - Mn_2O_3$

It was found that upon prolonged oxidation in an aqueous environment cinnamon-brown Mn_3O_4 became progressively darker in color. Electron micrographs of this material showed crystals having a pseudocubic habit but generally less well developed and smaller in size than Mn_3O_4. *X*-ray patterns of samples taken periodically during the oxidation disclosed only the pattern of Mn_3O_4, but chemical analysis yielded oxygen contents as high as $MnO_{1.44}$. Simon (1937) reported a preparation having the Mn_3O_4 structure and the composition $MnO_{1.48} \cdot 0.15\ H_2O$. Moore, Ellis and Selwood (1950) found that a compound could be prepared which had the structure of Mn_3O_4 but was very close to MnOOH in composition. Verwey and de Boer (1936) prepared a compound having the structure of Mn_3O_4 but the composition $MnO_{1.50}$. They called this compound γ-Mn_2O_3. Drotschmann (1960) prepared a compound having the hausmannite structure and the composition $MnO_{1.39}$. He found, on the basis of magnetic susceptibility measurements, that this compound should contain only the divalent and tetravalent states of manganese.

An experiment was made in which a suspension of Mn_3O_4 was strongly oxidized with oxygen gas. Eh and pH were recorded during the oxidation. The *x*-ray pattern (Table 4) is identical with that of Mn_3O_4, with the exception of weakening and/or absence of some of the high angle reflec-

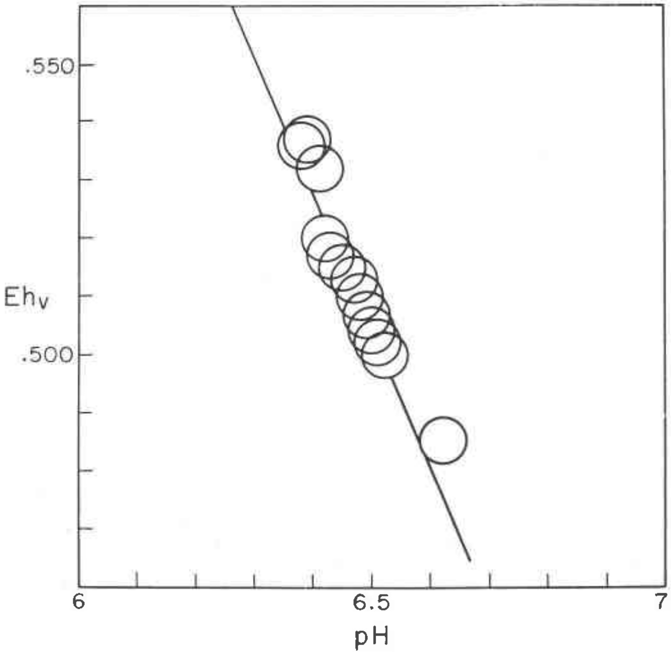

FIG. 5. Eh-pH response of Mn_3O_4 suspension. $a_{Mn^{2+}} = 2.34\times 10^{-3}$. Size of circles indicates precision of measurement.

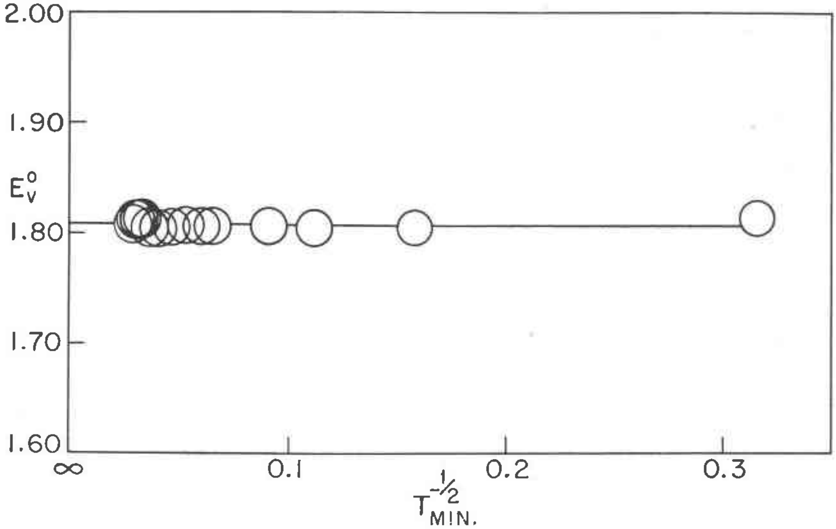

FIG. 6. Plot of E° vs. $T_{MIN}^{-1/2}$ for reaction $3Mn^{2+} + 4H_2O = Mn_3O_4 + 8H^+ + 2e$. Size of circles indicates limits of error of calculation.

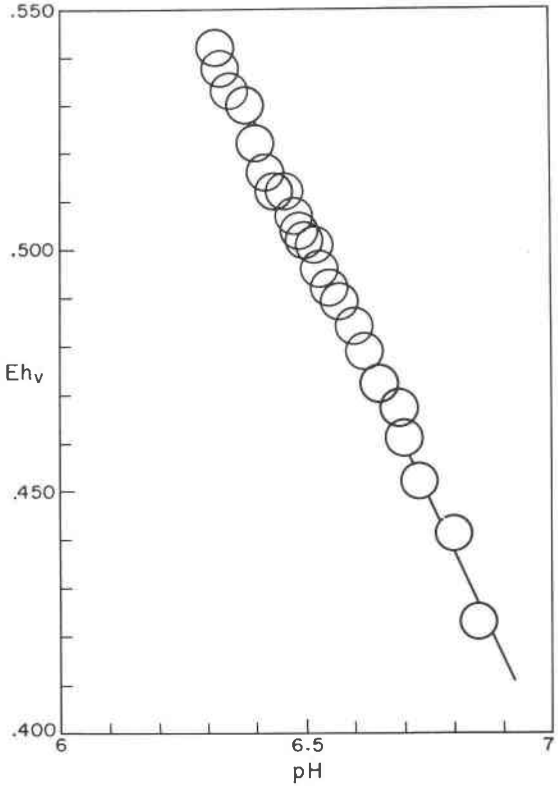

FIG. 7. Eh-pH response of Mn_3O_4 suspension. $a_{Mn^{2+}} = 4.68 \times 10^{-3}$. Size of circles indicates precision of measurement.

tions. Analysis of material prepared under similar conditions yielded the formula $MnO_{1.442 \pm .01} \cdot 0.49H_2O$, close to MnOOH. A plot of the Eh-pH curve (Fig. 9) shows that it has a slope of -0.177 pH corresponding to the reaction:

$$Mn^{2+} + 2H_2O = MnOOH + 3H^+ + e^- \qquad (16)$$

The potential is given by:

$$Eh = E^\circ - 0.177\ pH - 0.059 \log a_{Mn^{2+}} \qquad (17)$$

A plot of the E° potential of the reaction against the reciprocal of the square root of time (Fig. 10) is constant within the limits of experimental error at +1.548 v. The calculated free energy is -132.2 kcal. *X*-ray investigations showed that samples of γ-Mn_2O_3 kept in suspension for several months had partially inverted to γ-MnOOH, indicating that

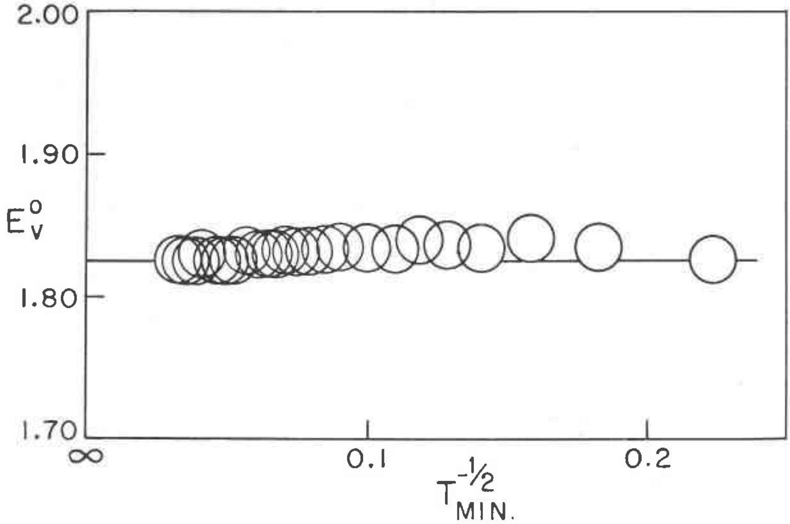

FIG. 8. Plot of E° vs. $T_{MIN}^{-1/2}$ for reaction $3Mn^{2+}+4H_2O=Mn_3O_4+8H^++2e$. Size of circles indicates limits error of calculation.

γ-Mn_2O_3 is unstable with respect to γ-MnOOH at 25° C. and one atmosphere total pressure.

In the course of these experiments it was assumed that the Mn^{2+} concentration in the solution remained constant after precipitation of the solid. In many cases fine precipitates are known to absorb ions from solution. Examination of equation (12) indicates that any change in the

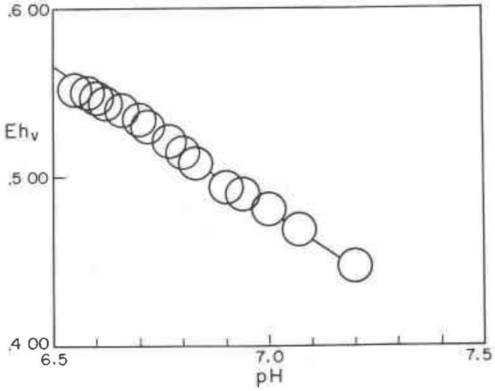

FIG. 9. Eh-pH response of γ-Mn_2O_3 suspension. $a_{Mn^{2+}}=1.48\times10^{-3}$. Size of circles indicates precision of measurement.

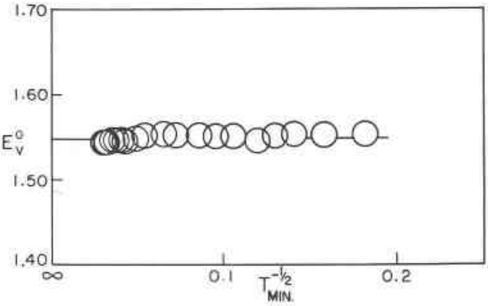

FIG. 10. Plot of E° vs. $T_{MIN}^{-1/2}$ for reaction $Mn^{2+}+2H_2O=\gamma\text{-}Mn_2O_3(MnOOH)+3H^++2e^-$. Size of circles indicates limits of error of calculation.

manganous ion concentration will be reflected by a change in the Eh or pH or both. On these grounds it was thought desirable to examine the variation in manganous ion concentration during the course of the oxidation reaction. The experimental apparatus was set up exactly as in previous runs; however, aliquots of solution were withdrawn after precipitation of $Mn(OH)_2$, before oxidation of the suspension, and periodically during the oxidation. Figure 11 shows the results of this experiment. It can be seen that the manganous ion concentration remains constant

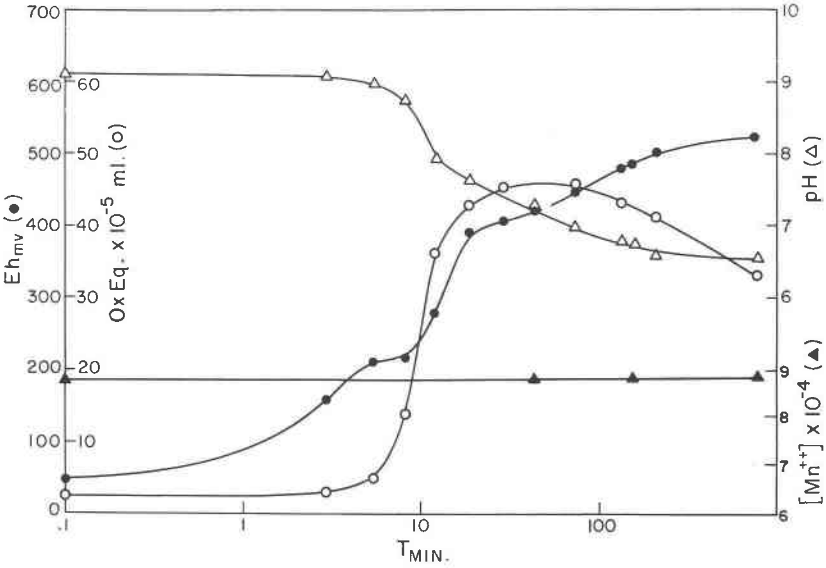

FIG. 11. Response of Eh, pH, oxidizing equivalents, and manganous ion concentration during oxidation of $Mn(OH)_2$ suspension.

within the limits of error of the analytical determination (Mn^{2+} was determined colorimetrically after oxidation to MnO_4^-).

The pH of the system, nearly constant before oxidation, decreased during the oxidation. The Eh of the system rose from its previously steady value. When the experiment was terminated, the Eh and pH had almost leveled out. The oxidizing equivalent of the system was determined colorimetrically using o-tolidine. It was essentially zero before oxidation, rose sharply during oxidation, then slowly decreased. This determination is a measure of the amount of manganese, with an oxidation state higher than 2+, present in the solid phase. Complete homogeneity of the system is therefore essential for an accurate determination. It was noted after a period of about thirty minutes that solid material was beginning to adhere to the electrodes and to the walls of the reaction vessel. Since the oxidized portion of the system is the solid phase, the oxidizing equivalent will appear to decrease as increasing amounts of solid adhere to the vessel, accounting for the apparent decrease in the oxidizing equivalent of the system after thirty minutes.

The Mn^{2+} concentration calculated from the stoichiometry of the precipitation reaction corresponds to the analytically determined Mn^{2+} concentration. There is no measurable adsorption of Mn^{2+} by the solid phase.

Hydrohausmannite

Feitknecht and Marti (1945) prepared a hydrous compound that had a manganese to oxygen ratio between Mn_3O_4 and MnOOH, by oxidation of an aqueous suspension of $Mn(OH)_2$. The *x*-ray diffraction pattern of this material was identical to that of hausmannite with the exception of a strong extra reflection in the low angle region and a general weakening of the intensities of the remaining reflections. They believed that this compound was a hydrated form of hausmannite, capable of some variation in manganese to oxygen ratio, and named it hydrohausmannite.

Frondel (1953) described a mineral from Franklin, N. J., that had an *x*-ray diffraction pattern identical to that of the compound prepared by Feitknecht and Marti. He indexed this pattern in terms of a tetragonal cell with $a = 5.79$ and $c = 9.49$ Å. Using the chemical analysis of bäckströmite (identical to hydrohausmannite) cited by Aminoff (1919) and the specific gravity of hausmannite, he calculated the approximate unit cell content to be $x = 1.155$ in the formula:

$$(\overset{II}{Mn}_{4-2x}\overset{III}{Mn}_x V_x)\overset{III}{Mn}_8 O_{16-x}(OH)_x$$

Feitknecht, Brunner and Oswald (1962) found that the material originally described by Feitknecht and Marti as hydrohausmannite was actually a mixture of two phases: β-MnOOH and Mn_3O_4. Electron micrographs of their synthetic hydrohausmannite disclose particles of two distinct morphologies: an equant morphology corresponding to Mn_3O_4 and a platy hexagonal morphology corresponding to β-MnOOH. β-MnOOH was prepared separately to provide *x*-ray and chemical data. The *x*-ray pattern is listed in Table 5. A partial chemical analysis of this material disclosed a manganese to oxygen ratio of $MnO_{1.48}$. No total analyses were made.

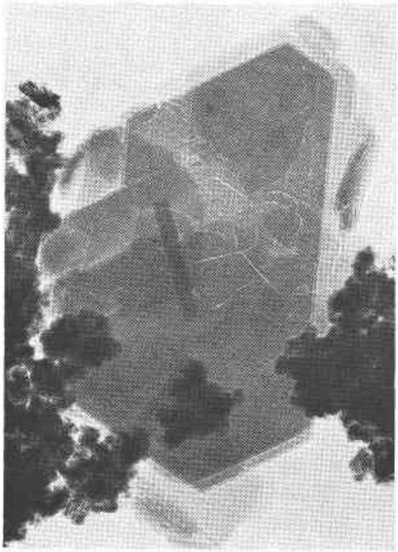

Fig. 12. Electron micrograph of synthetic hydrohausmannite. Large platelets are β-MnOOH; equant material Mn_3O_4. ×150,000.

Table 5 contains *x*-ray data for hydrohausmannite. A pattern of β-MnOOH is included for comparison. If the *x*-ray reflections of β-MnOOH are subtracted from the hydrohausmannite pattern, only the reflections of hausmannite remain.

1. *Experimental*

It was found that material having an *x*-ray pattern identical to natural hydrohausmannite could be prepared from dilute Mn^{2+} solution (≈ 0.001 m) by alkalization with NaOH in the presence of oxygen gas. Electron micrographs of this material disclosed two distinct morphological types; the one, platlets of hexagonal shape, the other equant in appearance (Fig. 12). The platy material is β-MnOOH, the equant material Mn_3O_4 and/or γ-Mn_2O_3. Material precepitated from highly oxygenated solution

TABLE 5. *X*-RAY DATA FOR HYDROHAUSMANNITE AND β-MnOOH

Hydrohausmannite Franklin, N. J. (Fondel, 1953)		Hydrohausmannite (Feitknecht and Marti, 1945)	
d	I	d[1]	I[1]
4.95	2	4.84	5
4.65	10	4.56	10
3.10	3	3.05	8
2.89	2	2.86	3
2.78	5	2.74	8
		2.67	4
2.50	6	2.47	8
2.38	4	2.36	6
2.05	3	2.02	6
1.844	1	1.84	5
1.803	2	1.78	4
1.710	1	1.69	4
1.655	1	1.63	4
1.586	5	1.56	7
1.549	4	1.53	6
1.447	2	1.43	7

Hydrohausmannite (This Work)		β-MnOOH (Feitknecht)		β-MnOOH (This Work)	
d	I	d[1]	I[1]	d[2]	I
4.90	2	4.61	S	4.62	10
4.62	10				
3.08	3				
2.87	2				
2.75	4				
2.65	2	2.67	M	2.64	5
2.48	4				
2.37	4	2.37	M	2.36	2 broad
2.03	2				
1.84	2	1.84	M	1.96	1 broad
1.79	1				
1.70	1				
1.57	4	1.56	M	1.55	
1.54	4			1.50	
1.44	3				
1.27	2				
1.23	1				

[1] Measured from a line diagram kindly provided by W. Feitknecht.

[2] All of the reflections on this pattern are broad; the two so marked are very broad.

has a manganese to oxygen ratio of $MnO_{1.50}$, indicating that the equant material in the mixture must be γ-Mn_2O_3 (β-MnOOH has not been observed with an oxygen to manganese ratio exceeding $MnO_{1.50}$). Materials precipitated from less highly oxygenated solutions have oxygen to manganese ratios between $MnO_{1.33}$ and $MnO_{1.50}$. Precipitation of this mixture appears to take place directly from solution. The low pH (≈ 7) at which precipitation occurs, however, suggests that there is local supersaturation with respect to $Mn(OH)_2$ around the drops of base at the instant they enter the solution. This causes precipitation of $Mn(OH)_2$ which is immediately oxidized to a mixture of Mn_3O_4 and β-MnOOH. Slow oxidation of $Mn(OH)_2$ produces only Mn_3O_4 as shown above. Apparently, the slow oxidation allows time for the complete transformation of the brucite-type layer structure of $Mn(OH)_2$ into the tetragonally distorted spinel structure of Mn_3O_4. The structure of β-MnOOH appears, from morphologic and x-ray data, to be closely related to the $Mn(OH)_2$ structure (Fig. 13). The lattice of β-MnOOH is quite distorted as indicated by the broadness of the x-ray reflections. The basal spacing has contracted from 4.72 Å in $Mn(OH)_2$ to 4.62 Å in β-MnOOH as a consequence of the increase in charge of all of the manganese ions from 2+ to 3+ (or one-half of the manganese ions from 2+ to 4+) and a loss of protons from the structure. A complete series of compounds spanning the composition range between $Mn(OH)_2$ and β-MnOOH very likely exists, although preparation of the less highly oxidized members has not been attempted. This series can be represented by the formula:

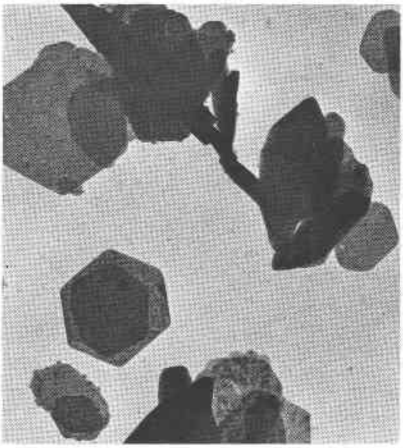

FIG. 13. Electron micrograph showing hexagonal platelets of β-MnOOH. ×80,000.

$$Mn^{II}(OH_2) \rightleftharpoons (Mn^{II}_{1-x}Mn^{IV}_{x})(OH_{2-2x}O_{2x}) \rightleftharpoons \beta\text{-}MnOOH \qquad (19)$$

in which the divalent manganese is oxidized to the trivalent state (or statistical distribution of 2+ and 4+, giving an average of 3+) and half of the protons migrate out of the structure.

A mixture of β-MnOOH and Mn_3O_4 is always formed upon rapid oxidation of and $Mn(OH)_2$ suspension. Supergene oxidation of pyrochroite at the Noda-Tamagawa mine, Japan, also produces a mixture of Mn_3O_4 and β-MnOOH consistent with the laboratory observations. Upon standing for long periods of time (several months) in contact with oxygen, aqueous suspensions of Mn_3O_4 and β-MnOOH invert to γ-MnOOH.

FIG. 14. Electron micrograph of Mn_3O_4 partially oxidized to γ-MnOOH (needles). ×80,000.

γ-Mn_2O_3 also inverts to γ-MnOOH upon standing for long periods in an aqueous environment (Fig. 14, 15). Preparation of a pure sample of β-MnOOH from aqueous solution was not possible in the range of conditions used in this work. Some Mn_3O_4 or γ-Mn_2O_3 was always formed along with the β-MnOOH. In order to prepare a pure sample of β-MnOOH for *x*-ray work and chemical analysis, it was necessary to oxidize $Mn(OH)_2$ in a stream of oxygen at low humidity (Feitknecht *et al.* 1962). The instability of β-MnOOH made it impossible to obtain free energy data by the method used in this study.

X-ray examination of hydrohausmannite from Långban, Sweden, yielded data identical to that obtained for synthetic hydrohausmannite (Table 5). A sample of material from Långban was ground in an agate mortar and examined by electron microscopy. (Fig. 16). The shape of the fragments produced by grinding depends to a large degree upon the cleavage of the material involved. In this case the morphologic types are much less distinct than in the synthetic material that was prepared in an environment allowing free growth of external crystal faces. Nevertheless, the same two morphologic types can be distinguished as in the synthetic material. Hydrohausmannite is a mixture of two phases, β-MnOOH and Mn_3O_4, and is not a valid mineral species. The name feitknechtite is here proposed for naturally occurring β-MnOOH, after Dr. Walter Feitknecht, Professor of Chemistry at the University of Bern, who first synthesized this compound and who has made many valuable contributions to the chemistry of the manganese oxides.

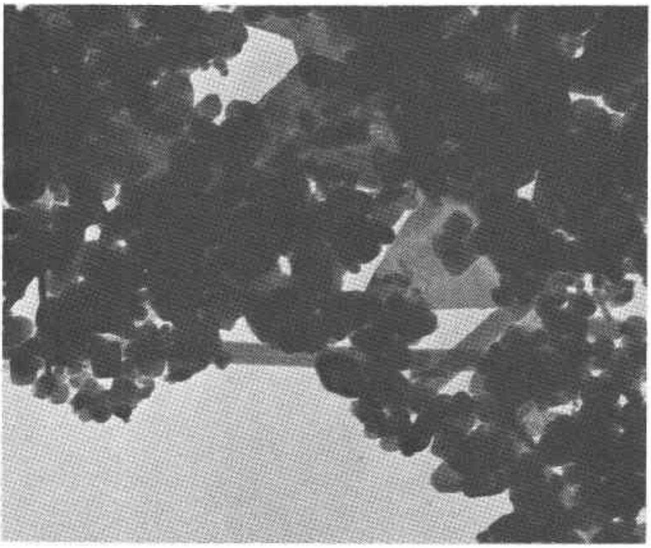

FIG. 15. Electron micrograph of γ-Mn_2O_3 (equant) and β-MnOOH (platy) partially altered to γ-MnOOH (needles). ×80,000.

Manganite

Manganite was first reported by de Lisle in 1772. It has space group $B2_1/d$ and unit cell dimensions $a=8.88$, $b=5.25$, $c=5.71$ Å (Buerger, 1936). The unit cell contains $Mn_8O_8(OH)_8$. Manganite is pseudoorthorhombic with $\beta=90°$. The structural analysis by Buerger is based upon trivalent manganese occupying sites in a sheet-like framework of oxygen and hydroxyl ions. Manganite has a superstructure of the marcasite type which exists up to the decomposition temperature of the compound (Dachs, 1962). Krishnan and Banerjee (1939) found that the magnetic anistropy data for manganite indicated non-equivalent oxidation states for the manganese atoms. They suggested that half of the manganese atoms had an oxidation state of 2+ and the other half 4+, giving an overall average of 3+ for the compound. In an investigation of manganite using both x-ray and neutron diffraction methods, Dachs (1963) has verified the earlier crystallographic work of Buerger, giving refined atomic parameters, and shown that the hydrogen ions are bound to cer-

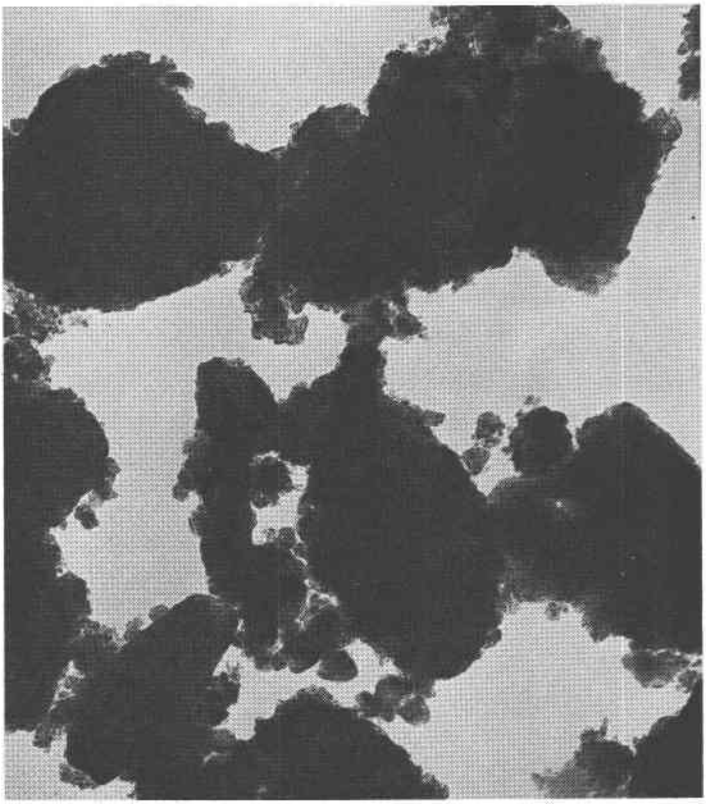

FIG. 16. Electron micrograph of hydrohausmannite from Långban, Sweden. Platelets (larger grains) are β-MnOOH; equant material Mn_3O_4. ×80,000.

tain oxygens in the structure. On the basis of his study he concluded that the existence of mixed oxidation states (2+ and 4+) among the manganese atoms in this compound is highly improbable. The writer favors the conclusion of Dachs.

Manganite occurs as a low temperature hydrothermal mineral and is commonly found in deposits formed by meteoric waters (Palache *et al.* 1955). It is the stable polymorph of MnOOH at 25° C. and one atmosphere total pressure.

1. *Preparation*

γ-MnOOH has been prepared by several investigators. Klingsberg (1958) prepared γ-MnOOH hydrothermally. Feitknecht and Marti (1945) prepared γ-MnOOH from manganous salt solutions by precipitation with ammonia in the presence of hydrogen peroxide. They obtained a product similar to manganite, but the *x*-ray pattern contained an additional weak low-angle reflection. Moore, Ellis and Selwood (1950 prepared γ-MnOOH by precipitation with ammonium hydroxide from a manganous sulfate solution in the presence of hydrogen peroxide, followed by drying at 60° C. under vacuum. In this study, γ-MnOOH was prepared by oxidizing a suspension of $Mn(OH)_2$ with hydrogen peroxide. A comparison of the *x*-ray data for this material and other synthetic and natural manganites is given in Table 6. Electron micrographs of this material show well formed crystals having a bladed habit (Fig. 17). It was found that under prolonged oxidation with air or oxygen, a suspension of $Mn(OH)_2$ oxidizes first to Mn_3O_4, then to γ-Mn_2O_3, and finally γ-MnOOH begins to form. If the initial oxidation is very rapid, some β-MnOOH is also formed.

Complete conversion of Mn_3O_4 to γ-MnOOH with air or oxygen alone could not be accomplished over the duration of the experiments. Feitknecht et al (1962) report that complete conversion of a mixture of Mn_3O_4 and β-MnOOH to γ-MnOOH occurs after four months of oxidation with oxygen gas. A number of other methods for the preparation of γ-MnOOH can be found in the literature; however, the products obtained are not sufficiently characterized to substantiate these methods.

2. *Free Energy of Formation of γ-MnOOH*

Few data on the free energy of formation of γ-MnOOH are available in the literature. Wadsley and Walkley (1951) give the half cell:

$$MnO_2 + H^+ + e^- = MnOOH; \qquad \Delta F_r^\circ = -25 \text{ kcal.} \tag{20}$$

The free energy of this reaction was determined from electrode potential measurements. Calculation of the free energy of γ-MnOOH from this

TABLE 6. *X*-RAY DATA FOR MANGANITE AND γ-MnOOH

Manganite Ilfeld, Harz Germany (Ramdohr, 1956)		γ-MnOOH (Gattow, 1962)		γ-MnOOH (Feitknecht and Marti, 1945)		γ-MnOOH This Work	
d	I	d	I	d[1]	I[1]	d	I
3.41	vs	3.40	20	4.79	w	3.41	10
2.64	m	2.64	10	3.39	s	2.65	5
2.52	w	2.53	6	2.62	m	2.52	1
2.41	m	2.42	14	2.52	w	2.41	8
2.26	m	2.28	8	2.40	s	2.36	.2
2.18	m	2.20	8	2.27	m	2.28	3
1.77	m	1.79	12	2.19	m	2.20	3
1.70	s	1.71	7	1.78	w	1.781	2
1.66	w	1.67	16	1.70	w	1.710	.5
1.63	s	1.64	6	1.67	s	1.675	9
1.50	m	1.50	7	1.64	w	1.637	.1
1.43	m	1.44	7	1.50	w	1.502	1
1.32	m	1.43	3	1.44	s	1.435	1.5
1.29	vw	1.32	7	1.43	m	1.323	.5
1.28	vw	1.30	2			1.262	.2
1.26	vw	1.28	2			1.214	.2
1.24	vw	1.26	4			1.182	.1
1.21	vw	1.24	2			1.158	.1
1.18	m	1.21	4			1.139	.2
1.16	m	1.18	7			1.118	.1
1.13	s	1.16	6			1.099	.2
1.11	m	1.13	8			1.080	.1
1.10	m	1.11	6			1.015	.1
1.08	m	1.09	6			0.993	.1
1.03	m	1.08	6				
1.01	m	1.03	7				
0.990	m	1.02	3				
		1.01	7				
		.99	8				

[1] "d" values and intensities taken from a line diagram constructed using θ angles. (Feitknecht, pers. comm.)

equation, using the free energy value of β-MnO$_2$ listed by Mah (1960) yields a value of -136.3 kcal. Drotschmann (1951) gives data which permit calculation of a value of -136.6 kcal. as the free energy of formation of γ-MnOOH. Bode, Schmier and Berndt (1962) obtained value of -134.6 kcal. from electrode potential measurements.

In this study γ-MnOOH was prepared by the method described above, and the Eh and pH of the suspension were measured. Figures 18

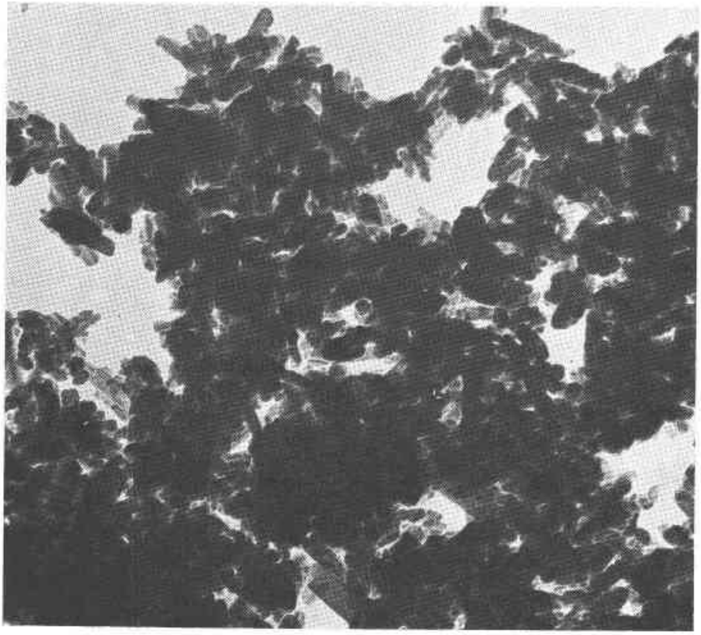

FIG. 17. Electron micrograph of γ-MnOOH. Crystals are well formed and have bladed habit characteristic of manganite. ×80,000.

and 20 show the Eh-pH response of two γ-MnOOH preparations.

An analysis of the product from the first experiment indicated an oxidation grade of $MnO_{1.51\pm.01}$. Determination of water by difference and recalculation of the analysis in terms of one Mn yields $MnO_{1.07}(OH)_{.89}$.

The E° values were calculated from the Eh-pH data using the reaction:

$$Mn^{2+} + 2\ H_2O = \gamma\text{-}MnOOH + 3H^+ + e^- \qquad (21)$$

The potential is given by:

$$Eh = E^\circ - 0.177\ pH - 0.059 \log a_{Mn^{2+}} \qquad (22)$$

Eh, pH and $a_{Mn}{}^{2+}$ are known; thus:

$$E^\circ = Eh + 0.177\ pH + 0.059 \log a_{Mn^{2+}} \qquad (23)$$

Figures 19 and 21 show E° as a function of the reciprocal of the square root of time. The respective E° values are 1.490 v. and 1.500 v. The free energy of formation of γ-MnOOH was calculated from these E° values and the free energy values of H_2O aq. and Mn^{2+} aq. listed by Latimer (1952).

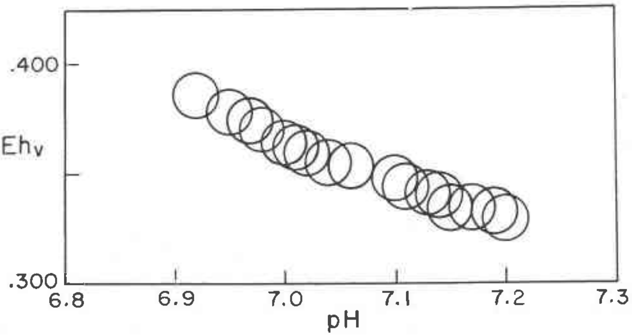

FIG. 18. Eh-pH response of γ-MnOOH suspension. $a_{Mn^{2+}} = 1.26 \times 10^{-2}$. Size of circles indicates precision of measurement.

From

$$\Delta F^\circ_r = n\mathfrak{F}E^\circ \tag{24}$$

and

$$\Delta F_{\gamma\text{-MnOOH}} = \Delta F^\circ_{Mn^{2+}\,aq.} + 2\,\Delta F^\circ_{H_2O\,aq.} + \Delta F^\circ_R \tag{25}$$

one obtains a value of -133.2 kcal. for the free energy of formation of γ-MnOOH. This is about three kilocalories less negative than the values reported by Wadsley and Drotschmann and slightly more than one kilocalorie less negative than the value of Bode *et al.*

The free energy values reported by Wadsley and Drotschmann were calculated using data obtained from battery investigations in which concentrated electrolyte solutions were employed. Estimation of activity coefficients in this type of system is uncertain. The value of Bode *et al.* is based on electrode measurements of the reaction:

$$\gamma\text{-MnOOH} = \beta\text{-MnO}_2 + H^+ + e^- \tag{26}$$

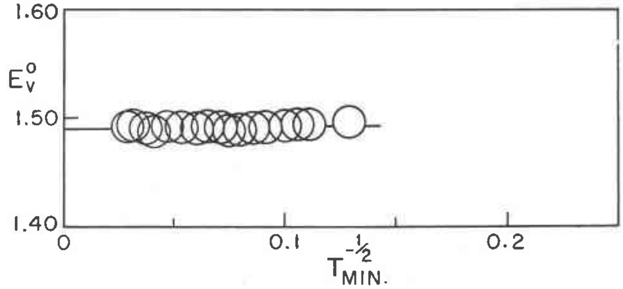

FIG. 19. Plot of E° vs. $T_{MIN}^{-1/2}$ for reaction $Mn^{2+} + 2H_2O = \gamma\text{-MnOOH} + 3H^+ + 2e^-$. Size of circles indicates limits of error of calculation.

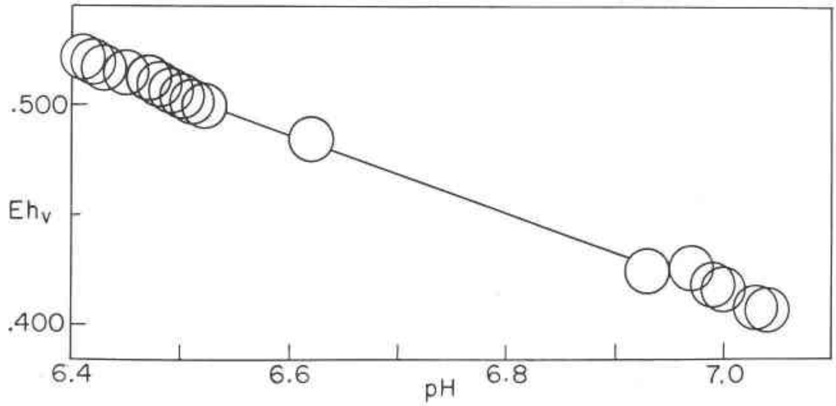

FIG. 20. Eh-pH response of γ-MnOOH suspension. $a_{Mn^{2+}}=2.34\times10^{-3}$. Size of circles indicates precision of measurement.

These measurements were carried out in an unbuffered saturated KCl solution, open to the atmosphere, with an initial pH of 6.4. The method used to determine the pH of the KCl solution was not specified. Measurement of pH in saturated salt solutions is subject to large errors. The E° potential of reaction (26) is a function of pH; thus the free energy value of γ-MnOOH determined by this method is questionable.

Schmalz (1959) found that the free energy of hydration for the reaction:

$$Fe_2O_3 + H_2O = 2\ FeOOH \tag{27}$$

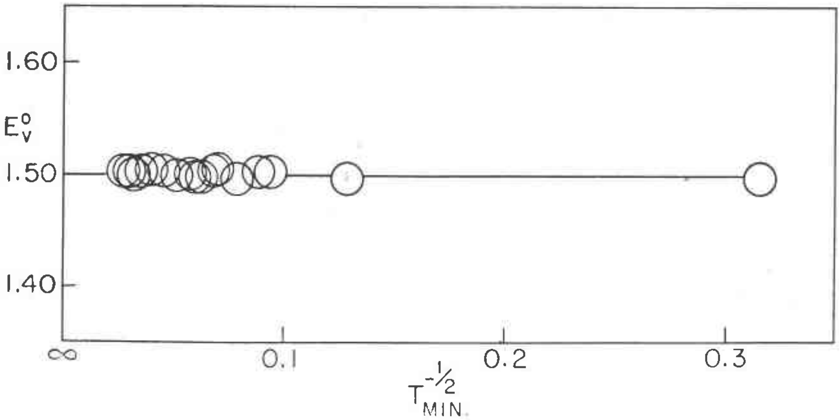

FIG. 21. Plot of E° vs. $T_{MIN}^{-1/2}$ for reaction $Mn^{2+}+2H_2O=\gamma\text{-}MnOOH+3H^++e^-$. Size of circles indicates limits of error of calculation.

was on the order of 0.1 kcal. Assuming no free energy of hydration for the reaction

$$Mn_2O_3 + H_2O = 2\ MnOOH \qquad (28)$$

and using the free energy value of Mn_2O_3 listed by Mah (1960) and the free energy value of H_2Oaq. listed by Latimer (1952), one obtains −133.27 kcal. as the free energy of formation of γ-MnOOH. The experimentally determined free energy value of γ-MnOOH (-133.3 ± 0.2 kcal.) indicates that the hydration energy of reaction (23) is less than 0.2 kcal. This is the same order of magnitude as the hydration energy of the analogous iron system.

δ-MnO_2.

McMurdie (1944) described an artificial manganese dioxide that gave an *x*-ray diffration pattern consisting of two lines. He believed it to be a distinct species and proposed the name δ-MnO_2 for this compound. Feitknecht and Marti (1945) prepared compounds varying in composition between $MnO_{1.74}$ and $MnO_{1.82}$ by oxidation of ammoniacal aqueous suspensions of manganous hydroxide with hydrogen peroxide, and between $MnO_{1.82}$ and $MnO_{1.96}$ by reduction of $KMnO_4$ solutions with HCl or hydrogen peroxide. These compounds all gave similar *x*-ray patterns; however, some contained more reflections than others. Feitknecht and Marti called the compounds manganous manganites and considered them to be double-layer compounds with varying degrees of order. They suggested that these compounds could be represented by the formula $4MnO_2 \cdot Mn(OH)_2 \cdot 2H_2O$. The *x*-ray patterns corresponded to McMurdie's δ-MnO_2 but for the most part contained additional lines. Cole *et al.* (1947) and Copeland *et al.* (1947) found that air oxidation of alkaline manganous solutions yielded a product with an *x*-ray pattern identical to manganous manganite. The compounds prepared by Copeland *et al.* varied in oxidation grade between $MnO_{1.80}$ and $MnO_{1.96}$. McMurdie and Golovato (1948) reported a synthetic δ-MnO_2 that gave an *x*-ray pattern containing two reflections in addition to the two they had originally reported in 1944. They also reported a naturally occurring δ-MnO_2 in manganese ore from Canada. Buser *et al.* (1954) investigated the substances described as δ-MnO_2 and manganous manganite. They obseved that the *x*-ray pattern of products with an oxidation grade above $MnO_{1.90}$ consisted of only two reflections corresponding to the pattern of McMurdie's (1944) δ-MnO_2. *X*-ray patterns of products with an oxidation grade below $MnO_{1.90}$ corresponded to the patterns of manganous manganite described by Feitknecht and Marti. Although it was concluded that manganous manganite and δ-MnO_2 are the same phase, they recommended retaining both names, δ-MnO_2 to describe compounds with an oxidation grade above $MnO_{1.90}$, and manganous manganite to describe those with an oxidation grade below $MnO_{1.90}$. The well-crystallized compound prepared by Buser *et al.* supported the double layer structure proposed by Feitknecht and Marti and made it possible to index the *x*-ray pattern on the basis of a hexagonal unit cell with $a=5.82$ and $c=14.62$ Å. The absence of basal reflections from the *x*-ray patterns of the more highly oxidized compounds was attributed to a disordering of the structure as Mn^{2+} in the interlayer was oxidized to Mn^{3+} or Mn^{4+}. Surface area measurements by the B.E.T. method indicate surface areas on the order of 300 m^2/g for the δ-MnO_2 and 45 m^2/g for the manganous manganite (Buser and Graf, 1955). Conflicting results have been reported by Glemser and Meisiek (1957) who prepared a δ-MnO_2 with the oxidation grade $MnO_{1.93}$ that gave an *x*-ray pattern containing basal reflections (Table 7). Glemser *et al.* (1961) have discussed the preparation and properties of δ-MnO_2. They found that δ-MnO_2 with an oxidation grade up to $MnO_{1.99}$ could be prepared without the loss of the basal *x*-ray reflections, and divided the preparations into three subtypes (δ, δ', δ'') on the basis of the intensity and sharpness of the *x*-ray reflections. Each subtype was prepared over the full range of composition. Previous surface area measurements by McMurdie and Golovato (1948) of δ-MnO_2 prepared by the same method that was subsequently used by Glemser *et al.*, indicated surface areas on the order of 40 m^2/g. Apparently the presence or absence of basal reflections is a function of particle size rather than oxidation grade. The particle size of δ-MnO_2 showing no basal *x*-ray reflections is so small that the particles can be considered to be "two-dimensional" crystals attaining a thickness of only a few atomic layers. The δ-MnO_2 and manganous manganite preparations that display the basal reflections have surface areas of nearly an order of magnitude less than those not showing basal reflections.

Differences in the particle size of this compound are related to preparation procedures. On this basis it is suggested that the name manganous manganite be dropped and these compounds be referred to as δ-MnO_2. It is interesting to note that nearly identical *x*-ray patterns, with the exception of line width and line intensity, were obtained from preparations of δ-MnO_2 ranging in composition from $MnO_{1.74}$ to $MnO_{1.99}$.

Buser and Grütter (1956) found that δ-MnO_2 was one of the primary manganese compounds in deep sea manganese nodules. Jones and Milne (1956) described a new manganese mineral found in a fluvio-glacial gravel deposit near Birness, Scotland. It gave an *x*-ray pattern identical to δ-MnO_2 and analysis of an impure sample gave a formula close to

TABLE 7. X-RAY DATA FOR BIRNESSITE, MANGANOUS MANGANITE AND δ-MnO_2

Feitknecht and Marti (1945) Manganous Manganite		Buser *et al.* (1954) δ-MnO_2		Buser *et al.* (1954) Manganous Manganite		Glemser and Meisiek (1957) δ-MnO_2	
d[1]	I	d	I	d	I	d	I
6.9	s	2.43	s	7.2	s	7.2	8
3.49	w	1.42	s	3.63	m	3.6–3.7	2
2.39	m			2.43	s	2.42	7
1.67	m			1.42	s	2.12	2
1.49	w					1.62	2
						1.39–1.40	6

Jones and Milne (1956) Birnessite Birness, Scotland		Yo Hariya (1961) Birnessite Todoroki Mine, Hokkaido, Japan		This Work (1963) δ-MnO_2	
d	I	d	I	d	I
7.27	s	7.37	37	7.2	8
3.60	w	4.69	11	4.75	9
2.44	m	3.69	9	2.44	10
1.412	m	3.32	5	2.12	4 broad
		3.27	4	1.67	1 broad
		2.45	5	1.42	8 broad
		2.37	7	1.27	1
		2.09	5		
		1.41	8		

[1] Measured from line diagram.

$(Na_{0.7}\ Ca_{0.3})\ Mn_7O_{14}\cdot 2.8\ H_2O$. They named this mineral birnessite. Frondel *et al.* (1960) described birnessite from Cummington, Massachusetts, where it occurs as a product of the weathering and oxidation of manganese-rich rocks. Hariya (1961) reported an occurrence of birnessite in the Todoroki Mine at Hokkaido, Japan. Levinson (1962) found that birnessite was a major constituent of a shipment of manganese ore from a mine near Zacatecas, Mexico. Zwicker (pers. comm.) reports that birnessite is the first oxide formed in the oxidation of manganese carbonate rocks at Nsuta, Ghana. Birnessite is a low temperature manganese oxide formed by the supergene weathering and oxidation of rocks containing manganese.

1. *Free Energy of Formation of δ-MnO_2.*

In this study δ-MnO_2 was prepared by disproportionation of suspensions of Mn_3O_4. When a suspension of Mn_3O_4 is acidified, the following reaction occurs:

$$Mn_3O_4 + 4\ H^+ = MnO_2 + 2\ Mn^{2+} + 2\ H_2O \qquad (29)$$

It was found that mild acidification produced δ-MnO_2 and more intense acidification produced γ-MnO_2. Electron micrographs of δ-MnO_2 show material of platy appearance with very poorly developed crystal faces. Two preparations of δ-MnO_2 were made and the Eh and pH of the suspensions measured over a period of time. The results of these measurements are shown in Fig. 22 and 24. The slope of both Eh-pH curves is −0.118, which correspondes to the slope of the reaction:

$$Mn^{2+} + 2\ H_2O = MnO_2 + 4\ H^+ + 2\ e^- \qquad (30)$$

The potential is given by:

$$Eh = E^\circ - 0.118\ pH - 0.0295 \log a_{Mn^{2+}} \qquad (31)$$

Analyses of the preparations gave oxidation grades of $MnO_{1.75}$ for the first and $MnO_{1.81}$ for the second. Both preparations contained water; 9.1% and 6.5% respectively. It is apparent from the slope of the Eh-pH curve that reaction (30), or a similar reaction involving a hydrated product, is the potential determining reaction. Manganese ions with an oxidation state less than four, present in the solid phase, apparently behave as a diluent and influence the electrode potential only with respect to the E° obtained. E° values for both experiments were first calculated from equation (31) and plotted against the reciprocal of the square root of time (Figs. 23, 25). An attempt was then made to take into account the difference in E° produced by the diluent effect, assuming ideal solid solution behavior. A mole fraction term was added to equation (31) giving the following equation:

$$Eh = E^\circ - .118\ pH - .0295 \log \frac{a_{Mn^{2+}}}{\text{mole fraction } MnO_2} \qquad (32)$$

A new E° was calculated from equation (32). The E° of the $MnO_{1.76}$ was raised 0.003 v. and the E° of the $MnO_{1.81}$ was raised 0.002 v. It can be seen that the change in E° due to the diluent effect is within the limit of experimental error. The E°, and thus the free energy, of the solid phase does not show a strong dependency upon the amount of lower valent manganese it contains. The free energy of formation calculated from the data for $MnO_{1.76}$ and $MnO_{1.81}$ is, within experimental error, the free energy of the end member of the δ-MnO_2 series. The E° values obtained from equation (32) are +1.290 v. and +1.292 v. for the $MnO_{1.76}$ and

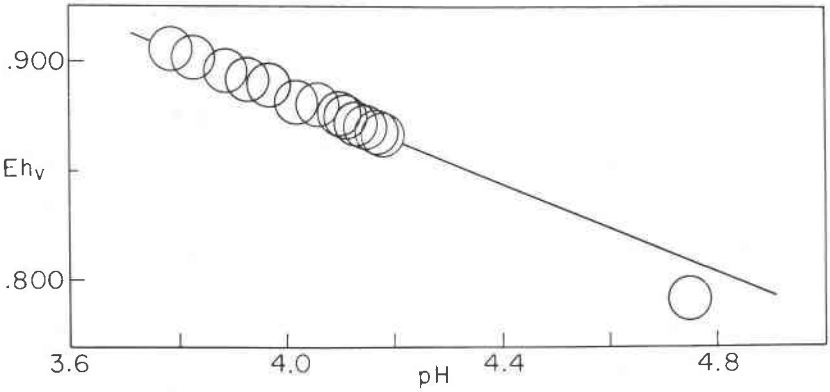

FIG. 22. Eh-pH response of δ-MnO_2 suspension. $a_{Mn^{2+}}=3.80\times10^{-3}$. Size of circles indicates precision of measurement.

$MnO_{1.81}$ respectively. The corresponding free energy values calculated from equation (30) using the free energy values of Mn^{2+} aq. and H_2O aq. listed by Latimer (1952) are −108.3±0.3 kcal. for $MnO_{1.76}$ and −108.2 kcal. for $MnO_{1.81}$. There are no free energy data available in the literature for δ-MnO_2.

The presence of significant amounts of cations other than manganese is characteristic of the chemical analyses of birnessite reported in the litera-

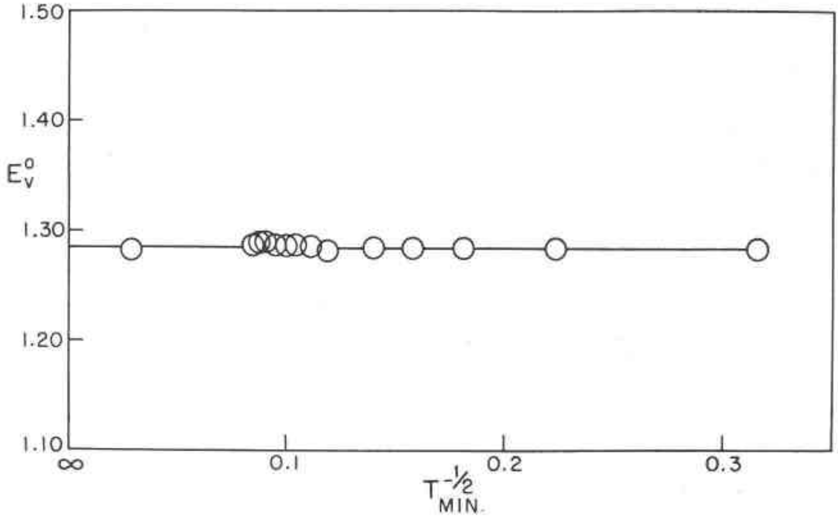

FIG. 23. Plot of E° vs. $T_{MIN}^{-1/2}$ for reaction $Mn^{2+}+2H_2O=\delta\text{-}MnO_2+44^{+}+2e^{-}$. Size of circles indicates limits of error of calculation.

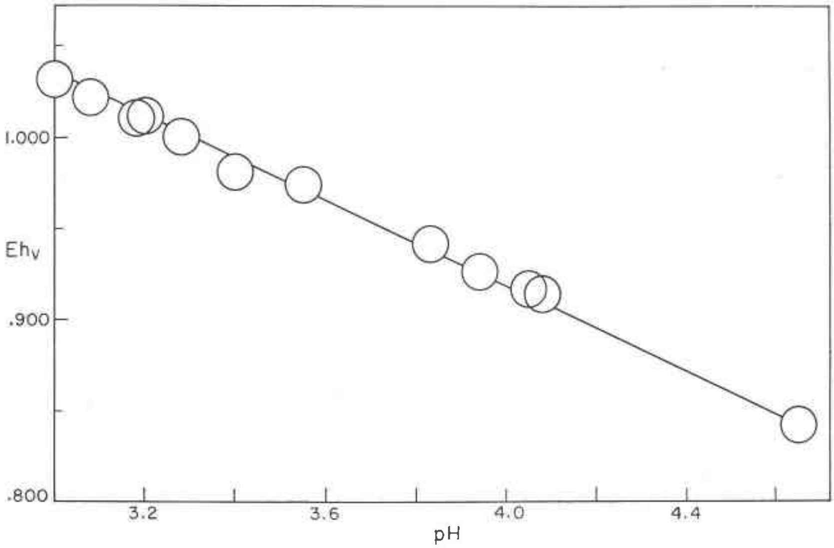

FIG. 24. Eh-pH response of δ-MnO_2 suspension. $a_{Mn^{2+}} = 4.26 \times 10^{-4}$. Size of circles indicates precision of measurement.

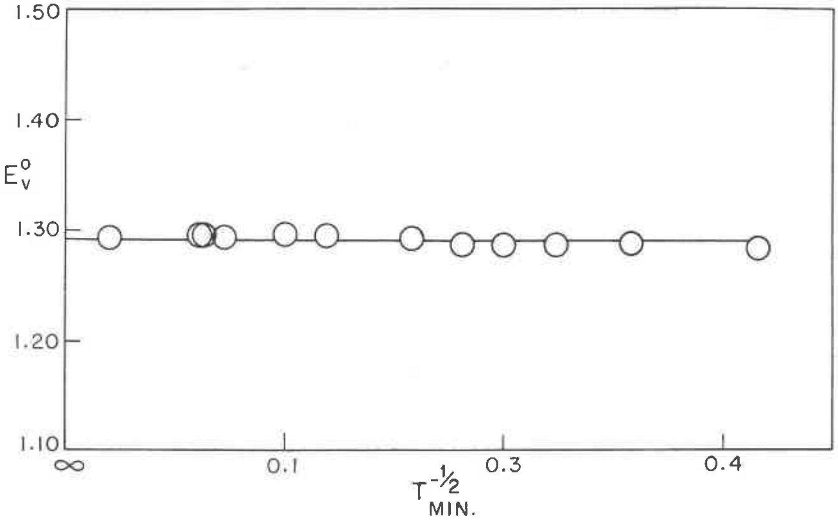

FIG. 25. Plot of E° vs. $T_{MIN}^{-1/2}$ for reaction $Mn^{2+} + 2H_2O = \delta\text{-}MnO_2 + 4H^+ + 2e^-$. Size of circles indicates limits of error of calculation.

ture. The type material described by Jones and Milne (1956) had clay minerals and other impurities admixed. The material Frondel *et al.* (1960) had available for analysis was limited in quantity and the presence of impurities was not discounted. It is reasonable to expect that a layer compound like birnessite could accommodate a large amount of other cations in its structure and the free energy of formation of the compound could be changed appreciably by their presence. A great deal more work needs to be done on the chemical composition of birnessite before the extent and the effect on free energy of incorporation of other cations into the structure can be fully evaluated. This study shows that the presence of other cations is not essential to the formation of δ-MnO_2, and the free energy reported is that of the pure end member.

Brenet *et al.* (1963) have attempted to describe the thermodynamic properties of all of the non-stoichiometric manganese dioxides in terms of the formula:

$$MnO_x(OH)_{4-2x} \tag{33}$$

According to their calculations, a manganese dioxide of composition $MnO_{1.76}$ would have a free energy of formation of −122.5 kcal. They believe that all of the manganese in the non-stoichiometric dioxides is in the tetravalent state and that reduction by oxalate (or other reducing agents) during chemical analysis occurs according to the process:

$$\overset{IV}{Mn}(1 - x/2)\overset{IV}{Mn}_{x/2}O_x(OH)_{4-2x} + x/2\ H_2C_2O_4 + H_2SO_4$$
$$\rightleftharpoons MnSO_4 + xCO_2 + 1/2(6 - x)H_2O + 1/4(2 - x)O_2(g) \tag{34}$$

In this reaction only the tetravalent manganese bonded to oxygen is reduced by oxalate (or other reducing agent), and the tetravalent manganese bonded to hydroxyl is reduced by water. In this manner they explain why analytical data for the non-stoichiometric manganese dioxides falsely indicate the presence of manganese in an oxidation state lower than 4+. The validity of their hypotheses rests upon whether or not manganese actually is present in these compounds in an oxidation state lower than 4+ and, if not, whether reaction (34) occurs. An examination of the standard analytical procedures for the analysis of manganese dioxide shows that a large excess of reducing agent is present in the system during the reduction, and the excess is then back-titrated to determine the quantity used in the reduction of the oxide. The potentials for the half cells:

$$H_2O \rightleftharpoons 1/2\ O_{2(g)} + 2H^+ + 2e^- \tag{35}$$

and

$$H_2C_2O_4 \rightleftharpoons 2\ CO_{2(g)} + 2H^+ + 2e^- \tag{36}$$

are +1.229 v. and −0.49 v. respectively. It would thus appear highly unlikely, even if the tetravalent manganese bonded to hydroxyl ion had a potential high enough to oxidize water, that it would preferentially oxidize water in the presence of an excess of oxalate. It is apparent from equation (34) that a certain amount of oxygen, varying as a function of x in the formula $MnO_x(OH)_{4-2x}$, should be generated when a non-stoichiometric oxide is reduced. No oxygen should be produced when stoichiometric MnO_2 is reduced. In order to test this hypothesis, a series of experiments was conducted in which δ-MnO_2 with an oxidation grade of $MnO_{1.90}$ and β-MnO_2 with an oxidation grade of $MnO_{2.00}$ were reduced with acidic Fe^{2+} solution in a manometric system. Identical analytical results are obtained when Fe^{2+} is employed as the reducing agent in place of oxalate. The half cell potential:

$$Fe^{2+} \rightleftharpoons Fe^{3+} + e^- \qquad E^\circ = +0.77 \text{ v.} \tag{37}$$

is less favorable than the oxalate potential for the reduction reaction. An increase in pressure for δ-MnO_2, amounting at maximum to 8.5% of the pressure increase predicted from equation (34) was observed. A similar increase was observed, however, for the β-MnO_2 which should have produced no oxygen according to equation (34). The observed change in pressure, whether or not due to generation of oxygen, is not a function of the composition of the oxide, nor could it account for the amount of deviation from stoichiometry observed in these oxides. After complete reduction of the oxides had taken place, it was noted that the solutions in which β-MnO_2 had been reduced were always more highly colored than the solutions in which δ-MnO_2 had been reduced, even though the same amount of oxide was used in each case. This is a qualitative indication that more of the ferrous iron was oxidized by β-MnO_2 than by δ-MnO_2 even though there was essentially no difference in the amount of gas produced by these oxides. The experiments do not prove that manganese in an oxidation state lower than 4+ is present in the non-stoichiometric dioxides; however, they do cast serious doubts on the hypothesis of Brenet *et al.*, which also fails to take into account the structural differences among the non-stoichiometric oxides. Such differences alone would appear to preclude the possibility of continuous variation of thermodynamic properties among these compounds.

The free energy value of δ-MnO_2 (−108.3 kcal.) determined in this study appears to be the best value available for this compound at the present time. δ-MnO_2 can vary in composition between $MnO_{1.74}$ and $MnO_{1.99}$, depending upon the conditions of the environment in which it formed and the conditions to which it was subjected after formation. The E° of reaction (32), and therefore the free energy of formation of δ-MnO_2, does not appear to be a sensitive function of the degree of compositional variation. Compositional variation in this compound is most likely due to the presence of Mn^{2+} or Mn^{3+} ions with the concomitant substitution of OH^- for O^{2-} to maintain electro-neutrality.

The range of composition of the compounds examined in this study is rather narrow. It would be desirable to investigate compounds over the entire compositional range shown by this compound.

γ-*MnO₂*

Dubois (1936) prepared a non-stoichiometric manganese dioxide with a manganese-oxygen ratio of $MnO_{1.88}$ that had an *x*-ray pattern differing from that of pyrolusite. Glemser (1939) prepared an oxide similar to that of Dubois by three different methods: oxidation of a boiling $MnSO_4$ solution containing KNO_3 with ammonium persulfate, oxidation of a boiling $MnSO_4$ solution containing KNO_3 with potassium permanganate, and decomposition of permanganic acid at 45° C. His products all gave identical *x*-ray diffraction patterns although they varied considerably in manganese-oxygen ratio ($MnO_{1.76}$, $MnO_{1.84}$, $MnO_{1.93}$). Boiling these compounds in nitric acid increased the ratio to $MnO_{1.97}$ in each case; however, no structural change was observed other than a sharpening of the reflections in the *x*-ray patterns. Glemser proposed the name γ-MnO_2 for this compound. McMurdie (1944) found that γ-MnO_2 was a major constituent of electrolytically produced MnO_2. Cole *et al.* (1947) distinguished three modifications of γ-MnO_2 on the basis of *x*-ray data. Gattow and Glemser (1961) have discussed the preparation and properties of γ-MnO_2.

Natural occurrences of γ-MnO_2 have been reported by Schossberger (1940), McMurdie and Galovato (1948), and more recently by Sorem and Cameron (1960) and Zwicker *et al.* (1962). The name nsutite was proposed by Zwicker *et al.* (1962) for naturally occurring γ-MnO_2 because of its abundance in the manganese deposits at Nsuta, Ghana. All of the reported occurrences of nsutite are consistent with a supergene origin of this oxide.

1. *X-ray Data*

There have been at least 21 different *x*-ray diffraction patterns of γ-MnO_2 published by different investigators (Gattow 1961). The *x*-ray data for some of the better characterized products are included in Table 8. The *x*-ray pattern of the material prepared in this study is identical to the pattern of manganoan nsutite with the exception of the absence of the weaker reflections. Preferred orientation and degree of crystallinity could account for the difference in the number of *x*-ray reflections observed by different investigators. It is apparent, however, that differences in the spacings of some reflections exist. Brenet *et al.* (1955) noticed that an expansion of the unit cell of γ-MnO_2 occurred during the first stage of discharge of a dry cell battery. Feitknecht *et al.* (1960) reduced γ-MnO_2 with hydrazine over the composition range $MnO_{1.96}$ to $MnO_{1.46}$ without a change of phase. They found that the unit cell volume increased linearly with decreasing x in MnO_x and suggested the mechanism:

$$MnO_2 + n\,e^- + n\,H^+ \rightleftharpoons MnO_{2-n}(OH)_n \tag{38}$$

whereby a part of the tetravalent manganese is reduced to a lower oxidation state and a corresponding number of oxygen atoms in the structure

TABLE 8. *X*-RAY DATA FOR NSUTITE, MANGANOAN NSUTITE, AND γ-MnO_2

Feitknecht (pers. communication) γ-MnO_2		Dubois (1963) $MnO_{1.88}$		Zwicker *et al.* 1962 Nsuta, Ghana				Zwicker *et al.* 1963	
				Manganoan Nsutite		Nsutite		γ-MnO_2	
d	I	d	I	d	I	d	I	d	I
4.01	M	4.	s	4.46	VW	4.36	VW	4.47	5
2.58	W	2.36	m	4.10	VS	3.96	VS	4.07	10
2.41	M	2.06	m	2.66	M	2.69	tr.	2.68	5
2.11	S	1.58	m	2.45	M	2.59	VW	2.45	9
1.63	VS	1.40	w	2.39	VW	2.43	S	2.36	5
1.43	M	1.38	w	2.36	M	2.34	M	2.16	8
1.38	M			2.16	S	2.22	VVW	2.13	2
				2.13	M	2.13	S	1.66	6
				1.924	VW	2.07	VW	1.43	1
				1.880	VVW	1.892	VVW	1.398	2
				1.667	S	1.831	tr.	1.08	1
				1.517	W	1.706	tr.		
				1.426	W	1.638	S		
				1.394	M	1.615	W		
				1.372	VW	1.488	VVW		
				1.330	W	1.425	W		
				1.292	VVW	1.362	VW		
				1.257	VW	1.306	VVW		
				1.225	VVW	1.250	tr.		
				1.187	VW	1.212	tr.		
				1.136	VVW	1.165	tr.		
				1.107	tr.	1.116	tr.		
				1.082	W	1.067	VW		

VVW = very, very weak, VW = very weak, W = weak, M = medium, S = strong, VS = very strong.

are bonded to protons forming hydroxyl groups, which maintains electroneutrality. The increase in cell volume is attributed to the larger size of lower valent manganese ions in the compound. Zwicker *et al.* (162) noted that the γ-MnO_2 from Ghana occurs in two modifications which they designated nsutite and manganoan nsutite. Sorem and Cameron had described a third type as well, characterized by the *x*-ray spacing 1.65 Å. Chemical analyses show that manganoan nsutite contains more lower-valent manganese than nsutite, and *x*-ray data indicate larger interplanar spacings in manganoan nsutite. They suggested that the observed differences in interplanar spacings are due to the larger amounts of lower-valent manganese in manganoan nsutite. Glemser *et al.* (1961) prepared three types of γ-MnO_2 (γ-MnO_2, γ-$'MnO_2$, γ-$''MnO_2$), varying only in the relative intensities and widths of the *x*-ray reflections in two cases, and the absence of one reflection in the third. No systematic shift in the spacings of the *x*-ray reflections was observed with variations in composition. Two γ-MnO_2 preparations were made in this study; one had an oxidation grade of $MnO_{1.91}$, the other $MnO_{1.99}$. No differences were observed in the *x*-ray spacings of these preparations.

2. *Free Energy of Formation of* γ-MnO_2

No free energy data have been published for γ-MnO_2. Wadsley and Walkley (1949) have measured the E° potentials of some γ-MnO_2 electrodes that varied in oxidation grade from $MnO_{1.92}$ to $MnO_{1.99}$. The measured potentials exhibited a large amount of scatter; however, a trend of decreasing potential with decreasing x in MnO_x was observed. All of the measured E° potentials were higher than the potential of the β-MnO_2 electrode. Bode *et al.* (1962) measured the potentials of γ-MnO_2 electrodes over the composition range $MnO_{2.00}$ to $MnO_{1.50}$ and found a linear decrease in potential with decreasing x in MnO_x. The design of their experiment did not permit the calculation of E° potentials from the measured electrode potentials; thus no free energy values could be calculated. Both investigations indicate that the free energy of formation of γ-MnO_2 varies as a function of the manganese-oxygen ratio, becoming more negative with decreasing x in MnO_x.

In this study γ-MnO_2 was prepared by the disproportionation of an aqueous suspension of Mn_3O_4 with acid. Electron micrographs show well developed acicular crystals (Figure 26). The Eh-pH response of the γ-MnO_2 preparation is shown in Fig. 27 and the corresponding E° potential in Fig. 28. In the second experiment a constant potential of 1.172 v. was measured at a pH of 1.51. The manganous ion activity was $10^{-1.91}$. This suspension was put into a bottle and sealed to determine whether aging effects were significant. After a year the bottle was opened and the

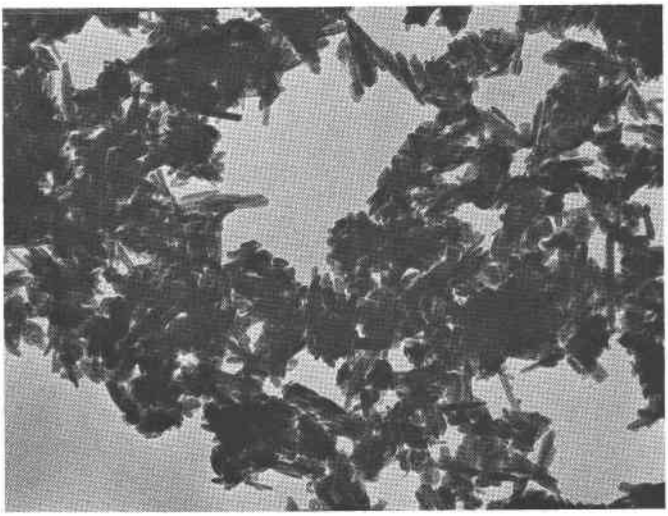

FIG. 26. Electron micrograph of γ-MnO_2 showing well developed acicular crystals. ×80,000.

Eh and pH measured. The pH had not changed, the Eh had increased 0.005 v. to +1.177 v., and the manganous ion activity was unchanged. The *x*-ray pattern of this material was identical to the original pattern before aging.

The slope of the Eh-pH curve is -0.118 as in the case of δ-MnO_2. Assuming the reaction:

$$Mn^{2+} + 2\ H_2O = MnO_2 + 4H^+ + 2e^- \tag{39}$$

the potential is given by

$$Eh = E^\circ - 0.118\ pH - 0.0295 \log a_{Mn^{2+}} \tag{40}$$

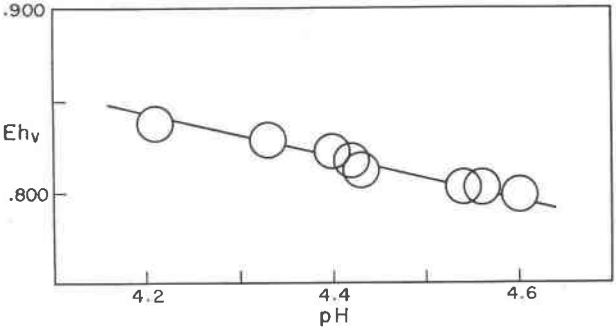

FIG. 27. Eh-pH response of γ-MnO_2 suspension. $a_{Mn^{2+}} = 6.92 \times 10^{-3}$. Size of circles indicates precision of measurement.

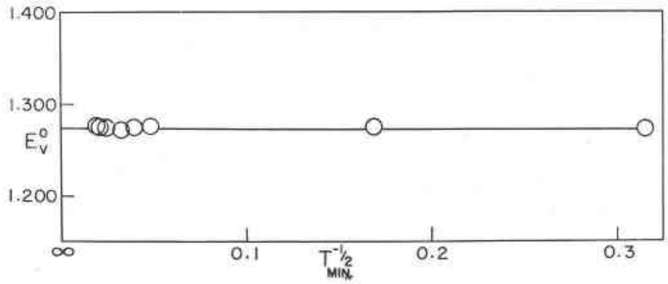

FIG. 28. Plot of E° vs. $T_{MIN}^{-1/2}$ for reaction $Mn^{2+}+2H_2O=\gamma\text{-}MnO_2+4H^++2e^-$. Size of circles indicates limits of error of calculation.

The activity of Mn^{2+} can be calculated from the manganous ion concentration using the Debye-Hückel approximation; Eh and pH are measured; thus E° can be calculated:

$$E^{\circ} = Eh + 0.118\ pH + 0.0295 \log a_{Mn^{2+}} \qquad (41)$$

A plot of E° as a function of the reciprocal of the square root of time is shown in Fig. 28.

The two preparations had manganese-oxygen ratios of $MnO_{1.91}$ and $MnO_{1.99}$ respectively. The corresponding E° values are +1.273 v. and +1.272 v. Free energy values calculated from these E° potentials and the free energies of Mn^{2+} aq. and H_2O aq. listed by Latimer (1952) are -109.12 ± 0.3 kcal. and -109.07 ± 0.3 kcal. respectively. Apparently the lower-valent manganese, causing deviation from stoichiometry in γ-MnO_2, behaves in an analogous manner to that in δ-MnO_2. The theoretical slope for reaction (39) or for a similar reaction involving a hydrated phase is observed. Treating the lower valent manganese as a diluent and recalculating E° using equation (32) does not change the E° of $MnO_{1.99}$ but increases the E° of $MnO_{1.91}$ to +1.273 v. The change in E° with composition over the range from $MnO_{1.91}$ to $MnO_{1.99}$ is within the error of measurements made using the technique described above. The free energy value of -109.1 ± 0.3 kcal. is, within the limit of experimental error, the free energy of formation of the pure γ-MnO_2 phase. It would be desirable to investigate γ-MnO_2 over its entire range of compositional variation to ascertain the relationship between E° and composition. It is conceivable that at some value of x in MnO_x the free energy curve of γ-MnO_2 might cross the free energy curve of β-MnO_2, reversing the relative stabilities of these compounds.

CONCLUSIONS AND GEOLOGIC APPLICATIONS

General. It has been found that a number of oxides and hydrous oxides of manganese can be prepared from aqueous Mn^{2+} solution. Techniques involve either direct precipitation or oxidation of suspended precipitates by the methods described above. These compounds are, in most cases, well crystallized as indicated by *x*-ray diffraction and electron microscopy. The measurement of pH and oxidation potential of aqueous suspensions of the oxides, when used in conjunction with values for the activity of manganous ion obtained through application of the Debye-Hückel approximation to manganous ion concentrations, permits calculation of free energy values. The free energy values determined in this study are in good agreement with published values in the few cases for which such data are available.

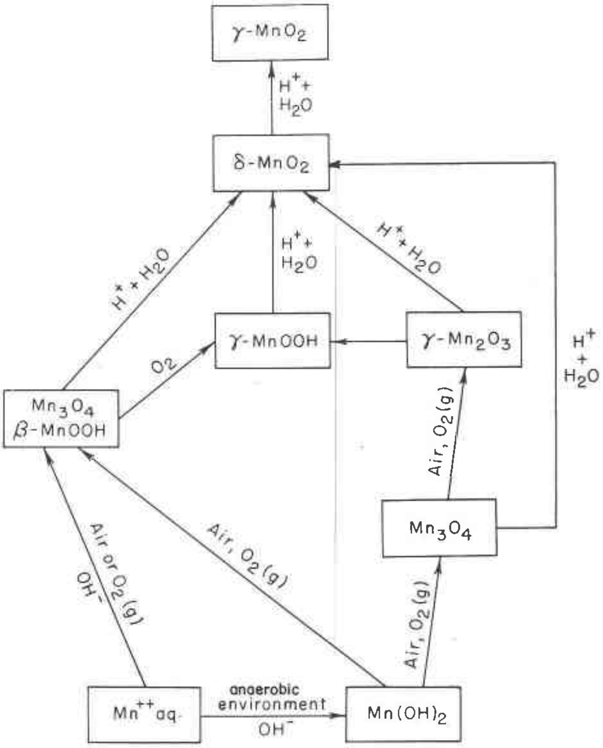

FIG. 29. Paths of reaction in the system Mn-O_2-H_2O at 25° C. and one atmosphere total pressure.

The paths of reaction in the laboratory synthesis of the manganese oxides are shown in Fig. 29. In every case, with the possible exception of the mixture of Mn_3O_4 and β-MnOOH formerly called hydrohausmannite, $Mn(OH)_2$ was precipitated first. It appears that direct precipitation of the Mn_3O_4-β-MnOOH mixture occurs; however, as drops of a strong base enter the Mn^{2+} solution, local supersaturation with respect to $Mn(OH)_2$ could cause precipitation of that compound. The $Mn(OH)_2$ would then be immediately oxidized, giving the appearance of direct precipitation of the more highly oxidized compounds. It was found that the most highly oxidized compound that could be synthesized using air, oxygen gas or hydrogen peroxide was γ-MnOOH. In order to prepare the non-stoichiometric forms of manganese dioxide, it was necessary to acidify suspensions of Mn_3O_4 or one of the MnOOH polymorphs. Upon acidification, disproportionation of these compounds into Mn^{2+} and non-stoichiometric MnO_2 occurs. The disproportionation reaction is a mechanism for penetrating the H_2O_2-O_2 barrier discussed by Sato (1960). Thus, it is apparent that all of these reactions can occur in the supergene environment in response to changing conditions of oxidation potential and pH.

A series of Eh-pH diagrams has been constructed to show the stability relations among the previously described phases. Although free energy data are available for manganosite and bixbyite, these phases were not included because they are not stable in the supergene environment. Groutite and ramsdellite cannot be included owing to the lack of thermochemical data. The free energy of formation of β-MnO_2 listed by Mah (1960) and the free energies of formation of H_2O aq. and Mn^{2+} aq. listed by Latimer (1952) have been used in addition to the free energy values determined in this study. Pyrolusite (β-MnO_2) has been included because it is apparently the most stable MnO_2 phase in the supergene environment, although it resists synthesis at 25° C. in the laboratory. In view of the decrease in potential of γ-MnO_2 electrodes with decreasing x in MnO_x observed by several investigators, it is conceivable that a reversal of the stabilities of γ-MnO_2 and β-MnO_2 might occur at some low value of x. Further investigation in this area is necessary. Figure 30 shows the least stable assemblage that would be expected in the supergene environment. Figure 31 shows the most stable assemblage of manganese oxides in the supergene environment. Figure 32 shows sections drawn at $pH=11$ indicating the changes in assemblage that would be expected with time. The free energy changes of the phase transitions are indicated. Figure 33 is an Eh-pH diagram constructed from previously existing thermochemical data and is included for comparison to the diagrams constructed from data determined in this study.

A number of thoroughly investigated supergene manganese oxide deposits have been formed by the oxidation of carbonate protore. Figures 34 and 35 are, respectively, the least and most stable assemblages of manganese oxides with rhodochrosite in equilibrium with groundwater containing a total dissolved carbonate activity of 10^{-2}. This value was chosen because it represents a reasonable approximation of the average total dissolved carbonate activity found in subsurface waters from carbonate bedrock (White *et al.*, 1963). Figure 36 shows the stable assemblage of oxides and carbonate in equilibrium with the atmosphere ($P_{CO_2} = 10^{-3.1}$). The free energy values of $CO_{3_{ag}}{}^{2-}$, $HCO_3{}^{-}aq.$, $CO_2(g)$, and rhodochrosite used in the construction of these diagrams were obtained from Latimer (1952).

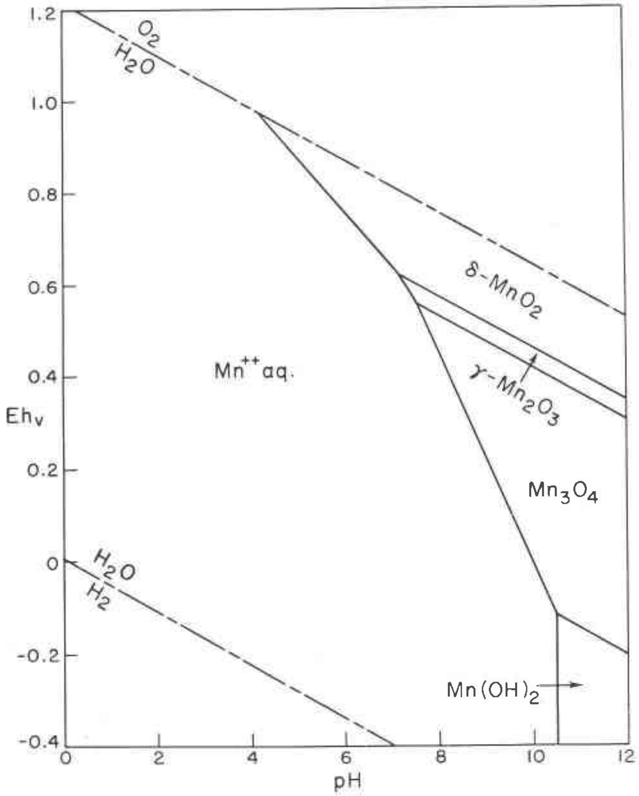

FIG. 30. Eh-pH diagram showing stability relations among some manganese oxides and pyrochroite at 25° C. and one atmosphere total pressure. Boundaries between solids and $Mn_{aq}{}^{2+}$ at $a_{Mn^{2+}} = 10^{-6}$.

Geologic Applications. Predictions have been made on the basis of the experimental data concerning the manganese oxide assemblages in the system $Mn\text{-}O_2\text{-}H_2O$ that should be found in supergene deposits. Owing to the fact that a number of the supergene oxides have only recently been described, detailed descriptions of occurrences of these minerals are limited. Six supergene manganese oxide deposits have been chosen in order to compare observed mineral assemblages with those predicted from experimental data.

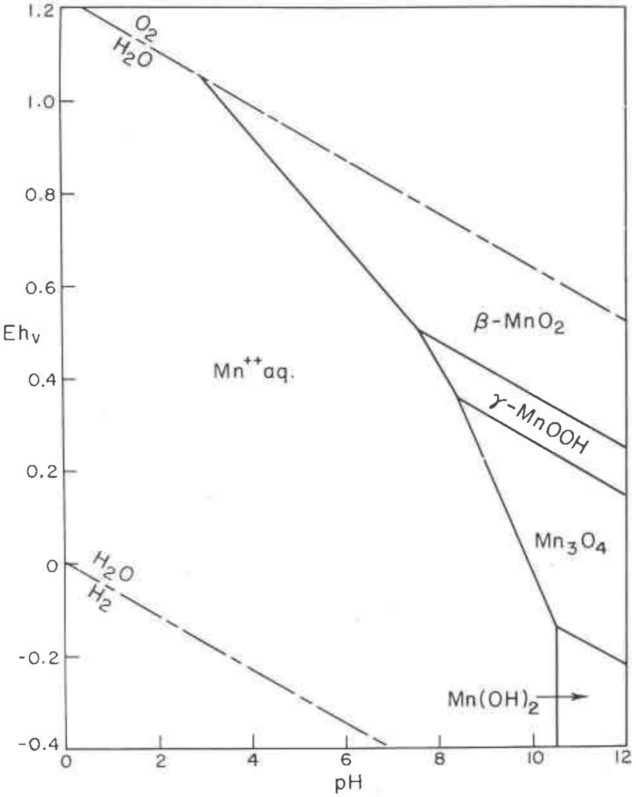

FIG. 31. Eh-pH diagram showing stability relations among some manganese oxides and pyrochroite at 25° C. and one atmosphere total pressure. Boundaries between solids and Mn_{aq}^{2+} at $a_{Mn^{2+}}=10^{-6}$.

At Minas Gerais, Brazil, protore consisting of manganese carbonate with some manganese silicates has been oxidized to depths of several hundred feet by supergene processes (Horen, 1953). Hausmannite is found in the protore-oxide contact zone and small amounts in the protore directly beneath the contact. In the oxide zone hausmannite is absent but pyrolusite, manganite, cryptomelane and one or more minerals that Horen grouped under the term "wad" are found. U. Marvin (pers. comm. found "γ-MnO_2 type" oxides in this deposit. Zwicker (pers.

comm.) identified birnessite, manganoan nsutite, and nsutite in the oxide zone adjacent to the protore. It is probable that these are the minerals Horen called "wad." The hausmannite (which may be primary, or may reflect the first stage of oxidation of the carbonate) and the non-stoichiometric dioxides are found near the carbonate-oxide contact; pyrolusite and cryptomelane are found in the oxide zone farther from the carbonate-oxide contact.

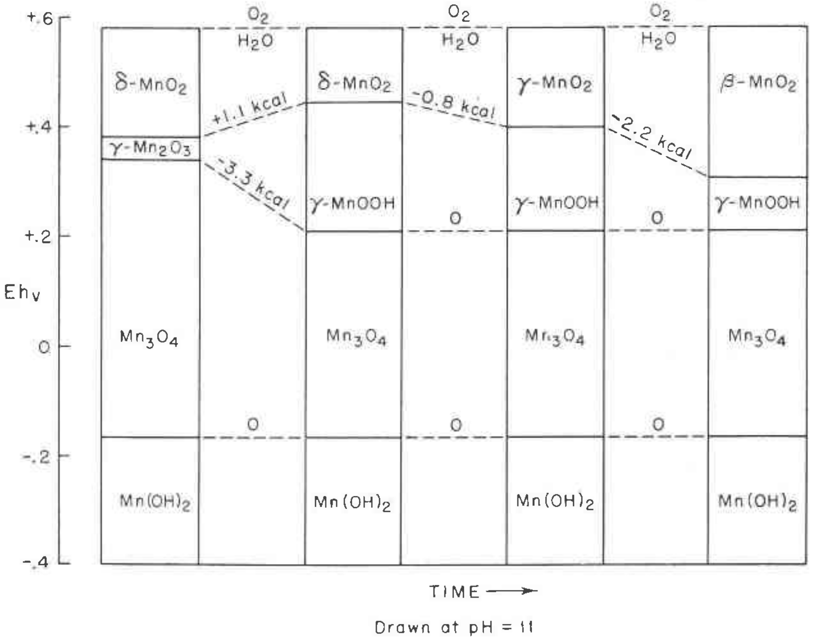

FIG. 32. Changes in mineral assemblage as a result of aging. Changes in free energies between polymorphs are indicated.

Baud (1956) in describing the manganese deposits at Moanda, French Equatorial Africa, writes:

> "La minéralisation se présente uniquement à proximité immédiate de la surface et elle affecte l'aspect d'une carapace épousant toutes les formes topographiques du terrain actuel. Grâce aux nombreux ouvrages de prospection foncés notamment dans la partie Nord du plateau Bangombé, il est possible de relever des coupes qui montrent la regularité et la continuité remarquables de cette carapace en dehors de certaines pentes trop brutales."

The protore at this deposit is bedded sedimentary rhodochrosite. Examination of the oxide-carbonate contact revealed that manganite is in contact with the protore (Jaffe and Zwicker, unpubl). The manganite forms a layer on the order of one millimeter in thickness and is overlain by pyrolusite (Fig. 37). Microscopic examination of the contact zone shows that the manganite and immediately adjacent pyrolusite have a common crystallographic orientation and that manganite is being pseudomorphously replaced by pyrolusite with progressive oxidation (Fig. 38). The equilibrium partial pressures of oxygen for each zone are indicated on the plates. The maximum thickness of oxides at this locality is approximately seven meters with the average being three to four meters. The assemblage of minerals found here is the most stable assemblage that one would expect to find in the supergene environment, on the basis of experimental data. Oxidation of the rhodochrosite has proceeded nearly to completion, and only a small amount of protore is left.

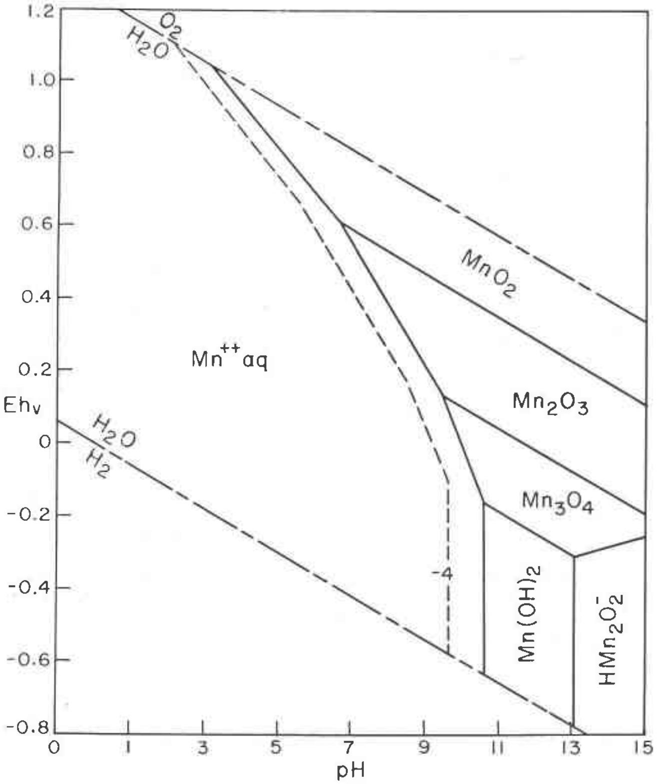

FIG. 33. Eh-pH diagram showing stability relations among some manganese oxides and pyrochroite at 25° C. and one atmosphere total pressure. Boundaries between solids and dissolved species at a dissolved species $= 10^{-6}$. Contour of $a_{Mn^{2+}}$ at 10^{-4}.

At Phillipsburg, Montana hydrothermally deposited rhodochrosite has undergone supergene oxidation into manganese oxides. The assemblage of minerals found in this deposit is manganite, birnessite, nsutite, cryptomelane and minor pyrolusite. Todorokite has also been described from this locality (Larson, 1962). A similar assemblage has been described from Butte, Montana where supergene oxidation of hydrothermal rhodochrosite has also occurred (Allsman, 1956). At Butte, nsutite appears to be the most abundant manganese oxide mineral. Allsman originally identified this mineral as ramsdellite, but subsequent investigation by Fleischer, Richmond and Evans (1962) have shown it to be nsutite. Pyrolusite is the next most abundant oxide, with cryptomelane being least abundant. The pyrolusite is found in open cavities and intimately mixed with nsutite. Cryptomelane is found in greatest

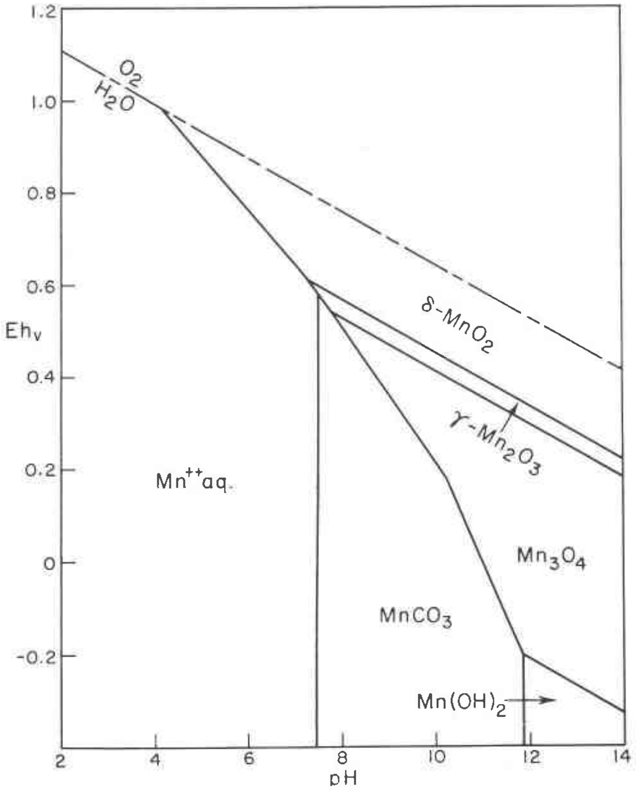

FIG. 34. Eh-pH diagram showing stability relations among some manganese oxides and manganese carbonate at 25° C. and one atmosphere total pressure. Boundaries between solids and Mn_{aq}^{2+} drawn at $a_{Mn^{2+}} = 10^{-6}$. Activity of total dissolved carbonate is 10^{-2}.

abundance where the potassium content of the circulating water is high.

The mineralogy of the manganese deposits near Piedras Negras, Mexico has been studied by Zwicker (pers. comm.).[1] At this locality argillaceous limestones and limey shales of low Mn content (<10% $MnCO_3$) have been weathered to depths of several inches to several feet leaving residual manganese oxides. The apparent oxidation sequence is: protore (dominantly carbonates containing Mn^{2+})→birnessite→oxidized form of birnessite→manganoan nsutite→nsutite. This sequence is identical to the sequence observed in the laboratory disproportionation of Mn_3O_4 or of the MnOOH polymorphs as a result of decreasing pH.

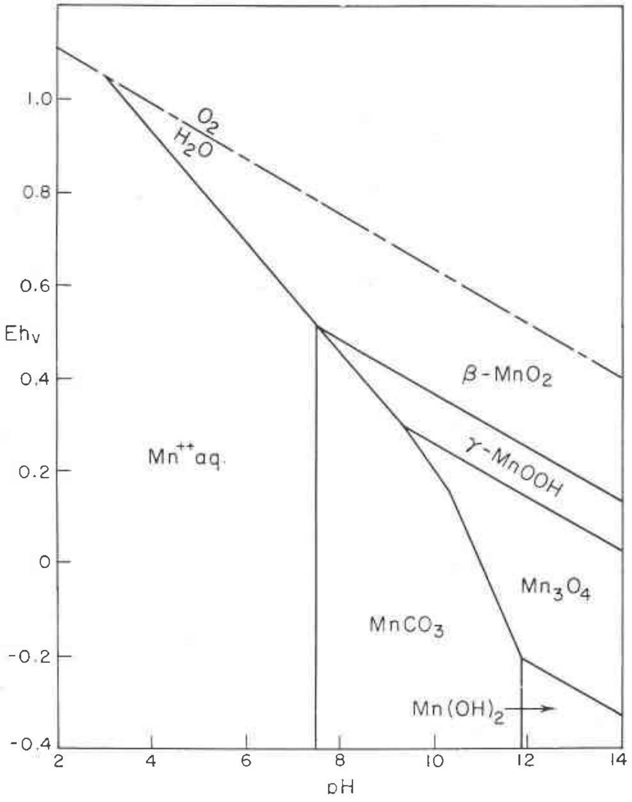

FIG. 35. Eh-pH diagram showing stability relations among some manganese oxides and manganese carbonate at 25° C. and one atmosphere total pressure Boundaries between solids and Mn_{aq}^{2+} drawn at $a_{Mn^{2+}} = 10^{-6}$. Activity of total dissolved carbonate is 10^{-2}.

---

[1] See also Levinson (1962).

A similar sequence has been observed in the manganese deposit at Nsuta, Ghana (Sorem and Cameron, 1960; Zwicker, unpubl.). The protore at Nsuta is sedimentary rhodochrosite. Supergene oxidation has proceeded to considerable depths forming a rich deposit of manganese oxides. The mineralogy is the same as that of the Mexican deposit except that pyrolusite and cryptomelane are present at Nsuta, and birnessite, found only near the carbonate-oxide contact, is much less abundant. Pyrolusite is found at the surface of the deposit. At shallow depths it is less abundant and is intimately mixed with nsutite.

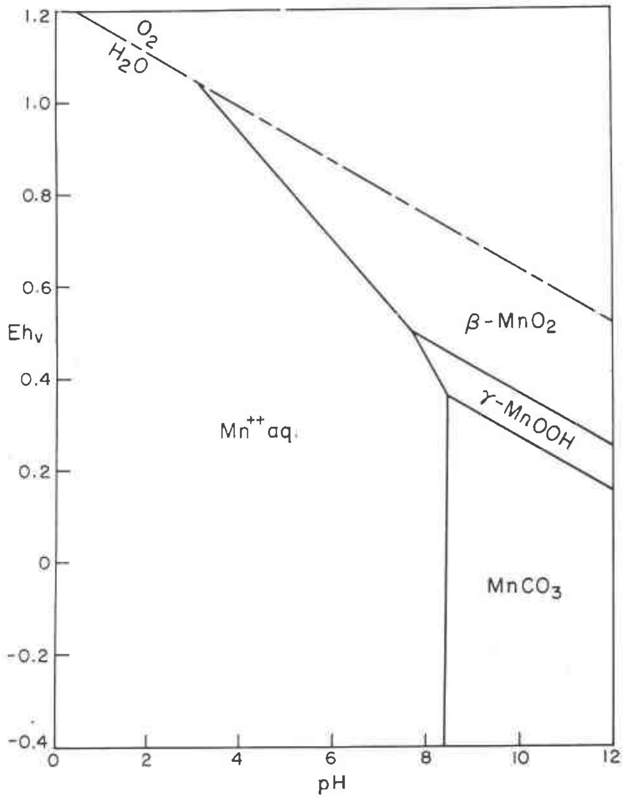

FIG. 36. Eh-pH diagram showing stability relations among some manganese oxides and manganese carbonate at 25° C. and one atmosphere total pressure. Boundaries between solids and Mn_{aq}^{2+} drawn at $a_{Mn^{2+}} = 10^{-6}$. P_{CO_2} is $10^{-3.5}$ atm.

The manganese deposit at Noda-Tamagawa, Iwate, Japan contains the largest known body of pyrochroite (Watanabe *et al.*, 1960). Over 50,000 tons of pyrochroite have been shipped from this locality for

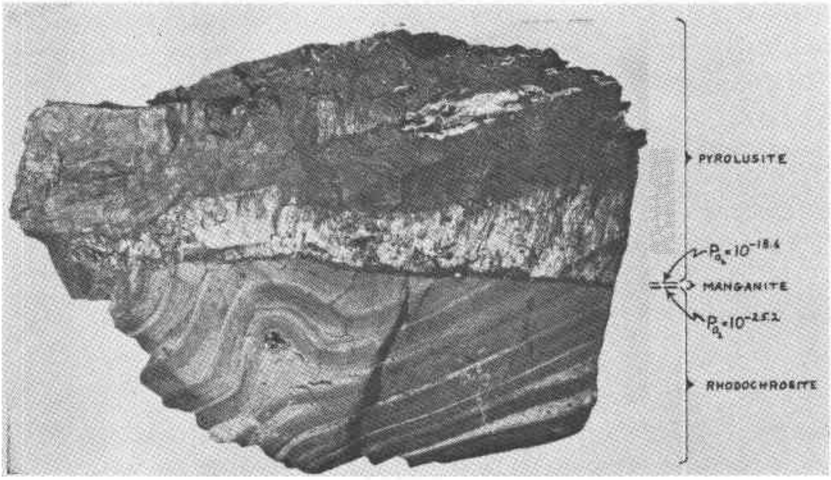

FIG. 37. Photograph of hand specimen from Moanda, French Equatorial Africa, showing contact between manganese oxides and sedimentary rhodochrosite (×2.3). Relict carbonate bedding persists into overlying oxide layer; contact represents downward limit of supergene oxidation. Partial pressures of oxygen at which phase transitions occur are indicated on plate. Courtesy of H. Jaffe, Union Carbide Nuclear Company.

metallurgical purposes since 1950. The pyrochroite is a hydration product of manganosite which apparently was formed by the metamorphism of sedimentary rhodochrosite. Hydration of manganosite took place either during the terminal stages of metamorphism, or at a later time as a

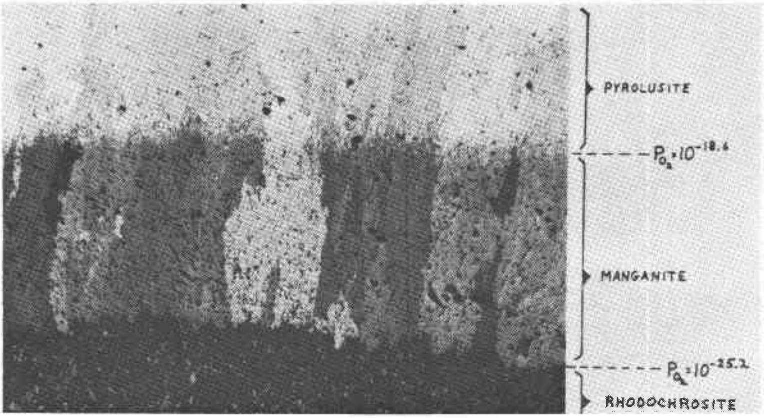

FIG. 38. Polished section of contact between rhodochrosite and manganese oxide. Rhodochrosite (dark gray) is oxidizing to manganite (medium gray) which is pseudomorphously replaced by pyrolusite (light gray). Partial pressures oxygen at phase transitions are indicated on plate. Courtesy of H. Jaffe, Union Carbide Nuclear Company.

result of descending supergene solutions. The upper portion of the deposit has been oxidized by supergene solutions and consists of pyrolusite, cryptomelane, ramsdellite,[1] and psilomelane. The first oxidation products of the pyrochroite are hausmannite and hydrohausmannite (Mn_3O_4 and β-MnOOH). Unfortunately, no data are available concerning the zone between the pyrochroite and the supergene oxide zones. It is likely that a thorough examination of this deposit would reveal the complete oxidation sequence from pyrochroite to pyrolusite.

In each of these deposits the sequence of oxides observed in passing vertically from the surface to the protore is similar. The compounds containing tetravalent manganese are found close to the surface or along channels which allow supergene waters or air free access to greater depths. Compounds containing only divalent manganese are found in the protore. Thus, a gradient in the average oxidation state of manganese in the oxides exists and is a function of the intensity of the oxidizing environment. The most important mechanisms involved in the oxidation process are the circulation of air through moist ore and protore and downward percolation of air-saturated meteoric water through the ore and protore. At localities where a high oxidation potential exists down to the protore contact, that is, either where the descending waters are replenished at a rate faster than they are depleted of their oxidizing capability, or circulation of air is rapid with respect to depletion of its oxygen content, a high average oxidation state of manganese will be found throughout the oxide zone. Where descending water is depleted of its oxidizing capability with depth or circulation of air is limited, a sequence of minerals will be observed, decreasing in average oxidation state with increasing depth or with decreasing accessibility to the oxidizing water or air.

Both of these mechanisms contribute to the oxidation of rhodochrosite deposits; however, an assessment of their relative importance indicates that circulating air must play the major role in the oxidation process. Typical ore from Nsuta, Ghana consists of nsutite, with small amounts of cryptomelane and pyrolusite. The moles of oxygen necessary to oxidize one mole of rhodochrosite to each of these oxides are given in Table 9. The value of X in the formula of nsutite is seldom higher than 0.05. Thus it can be seen that each of these reactions requires nearly $\frac{1}{2}$ mole of oxygen for each mole of rhodochrosite oxidized. The amount of oxygen necessary to produce one ton of this ore from rhodochrosite is approximately 4,000 moles, or 140 lbs. If air is the only source of oxygen, 670 lbs. would be required for each ton of ore produced. Under supergene condi-

---

[1] This paper was written before nsutite had been described, and the substance identified as ramsdellite might well be nsutite, as the *x*-ray patterns of these compounds are similar.

TABLE 9. OXYGEN REQUIREMENTS FOR SOME SELECTED REACTIONS

Reaction	Oxygen Required
1. $MnCO_3 + \frac{1}{2} O_2 = MnO_2 + CO_2$	$\frac{1}{2}$ mole O_2/mole $MnCO_3$
2. $8\,MnCO_3 + \frac{1}{2} K_2CO_3 + \frac{15}{4} O_2 = KMn_8O_{16} + \frac{17}{2} CO_2$	$\frac{15}{32}$ mole O_2/mole $MnCO_3$
3. $MnCO_3 + \frac{1}{2}(1 - x)O_2 + 2xH_2O$ $= \overset{IV}{Mn}_{1-x}\overset{II}{Mn}_x O_{2-2x}(OH)_{2x} + CO_2 + xH_2$	$\frac{1}{2}(1 - x)$ mole O_2/mole $MnCO_3$

tions, 670 lbs. of air occupy about 9,000 cubic feet. Thus the oxidation of one ton of protore would require the amount of oxygen contained in 9,000 cubic feet of air. One ton of protore has a volume of about 10 cubic feet. Assuming a porosity of 18%, it could contain 1.8 cubic feet of air. The complete oxidation of a given volume of protore would require about 5,000 complete changes of air. Assuming two changes of air per year, it would take about 2,500 years to oxidize one ton of protore, or, in terms of depth, an oxidation rate of approximately one foot per thousand years.

Consideration of the mechanism of oxidation by air saturated water shows that approximately 12,000,000 liters of water would be required to supply the oxygen necessary for complete oxidation of one ton of protore. About 420,000 cubic feet of air-saturated water would have to flow through each ten cubic feet of protore in the oxidation process. Again assuming a porosity of 18% and ideal permeability, each given volume of protore would have to be subjected to 230,000 complete changes of water.

Rainfall data are given in Table 10. If aerated water is the sole agent active in the oxidation process, it would require about 23,000 years to oxidize one ton of protore, assuming all of the rainfall in an area receiving 40″–60″ per year passed through the soil into the protore. Much rainfall

TABLE 10. RAINFALL DATA FOR SOME SELECTED LOCALITIES

Locality	Approximate Annual Rainfall[1]
Nsuta, Ghana	40″–60″
Moanda, French Equatorial Africa	60″–80″
Phillipsburg, Montana	10″–20″
Minas Gerais, Brazil	60″–80″

[1] Goode's World Atlas, 11th ed., 1960.

is lost in runoff and evaporation and oxygen losses occur when the water percolates through the soil zone. The time involved would therefore be somewhat longer. In excess of 2,000,000 years would be required to oxidize a rhodochrosite deposit to a depth of 200 feet. A prohibitive period of time would be necessary to produce a deposit such as the Nsuta ore body if the only oxidation mechanism were aerated water. The dominant mechanism in the formation of oxide ore bodies of this type must be the circulation of air.

It was not possible to synthesize manganosite, bixbyite, groutite, ramsdellite, or pyrolusite in the range of experimental conditions investigated. It is not surprising that manganosite and bixbyite could not be synthesized under supergene conditions because both of these minerals are found only in "dry" high temperature deposits. In the presence of water, manganosite is unstable with respect to pyrochroite and bixbyite is unstable with respect to manganite. Groutite and ramsdellite are found only in supergene deposits and pyrolusite is a common mineral in supergene deposits. Why these minerals are not amenable to synthesis under simulated supergene conditions remains a mystery. Attempts to synthesize groutite and ramsdellite under hydrothermal conditions have also failed (Klingsberg, 1958). Bode and Schmier (1962) claim to have synthesized ramsdellite by oxidation of γ-MnO_2, but their product is not well characterized nor are the conditions of synthesis stated. The thermal transformation of ramsdellite to pyrolusite (Ramsdell, 1932; Fleischer *et al.*, 1962); of groutite to ramsdellite (Klingsberg, 1958); and of δ-MnO_2 to γ-MnO_2 to pyrolusite (Glemser *et al.*, 1961; Gattow and Glemser, 1961) have been well demonstrated. Both δ-MnO_2 and γ-MnO_2 undergo thermal transformation into α-MnO_2 in the presence of high potassium concentrations (Faulring *et al.*, 1960). In view of the association of groutite, ramsdellite, and pyrolusite with supergene deposits, and the ease of thermal transformation among them, it is somewhat surprising that attempted synthesis at 25° C. and one atmosphere pressure have not succeeded. The temperatures necessary to effect the thermal transformations described above are not achieved in the supergene environment. Aging probably plays an important role in the formation of these minerals in nature.

ACKNOWLEDGMENTS

The author is indebted to Dr. Robert M. Garrels, of the Department of Geological Sciences at Harvard University, for his advice and aid both during the research and in the preparation of the manuscript. Dr. Clifford Frondel, of the Department of Geological Sciences, Harvard University, kindly provided mineral specimens for *x*-ray standards. Dr. Walter Zwicker, then of the Union Carbide Corporation, was particularly helpful in both the theoretical and technical phases of the study. The stimulating discussions with Mr. Howard Jaffe of the Union Carbide Corporation and his excellent advice on many problems that arose in the course of the study are gratefully acknowledged. Mr. W. Roettgers of the Union Carbide Corporation prepared the electron micrographs. Dr. Werner Stumm and Dr. James Morgan, Division of Engineering and Applied Physics, Harvard University, were very helpful with some analytical problems that arose in the research. Financial support for the investigation was kindly provided by the Union Carbide Ore Company.

REFERENCES

ALLSMAN, P. (1956) Oxidation and enrichment of the manganese deposits of Butte, Montana. *Mining Eng.* **11,** 1110–1112.

AMINOFF, G. (1919) Über Backströmit, eine rhombische Modifikation der Verbindung $Mn(OH)_2$. *Geol. För. Förh.* **41,** 473–491.

——— (1919) Über die Krystallstruktur des Pyrochroits. *Geol. För. Förh.* **41,** 407–430.

——— (1926) Über die Krystallstruktur von Hausmannit ($MnMn_2O_4$). *Zeit. Krist.* **64,** 475–490.

BAUD, L. (1956) Les gîsements et indices de manganese de L'Afrique Equatoriale Française. *XX Inter. Geol. Cong., Manganese Symp.* **2,** 9–38.

BERRY, L. G. AND R. M. THOMPSON (1962) X-ray powder data for ore minerals. *Geol. Soc. Am. Mem.* **85.**

BJERRUM, I., G. SCHWARZENBACH AND L. G. SILLEN (1958) Stability constants of metal-ion complexes, pt. 2 inorganic ligands. *Chem. Soc. London, Spec. Pub.* **7.**

BODE, H. AND A. SCHMIER (1962) Die "Synthese" des Ramsdellits. *Naturwissenschaften,* **49,** 465.

——— A. SCHMIER AND D. BERNDT (1962) Zur Phasenanalyse von Mangandioxyd. *Zeit. Electrochemie* **66,** 586–593.

BRENET, J. P. (1955) Batteries and accumulators. *Com. Inter. Thermodynam. Cinet. Electrochim., 7th Ann. Meet.* Butterworths, London, p. 299.

——— G. COEFFIER AND J. P. GABANO (1963) Étude analytique et thermodynamique de varietes de bioxyde de manganese. *Electrochem. Acta* **8,** 273.

BREWER, L., (1953) Thermodynamic properties of the oxides and their vaporization processes. *Chem. Rev.* **52,** 1–75.

BRITTON, H. T. S. (1925) Electrometric studies of the precipitation of hydroxides, part 1, precipitation of magnesium, manganous, ferrous, cobalt, nickel, and thorium hydroxides by use of the hydrogen electrode. *Jour. Chem. Soc.* **127,** 2110.

BUERGER, M. J. (1937) A common orientation and a classification for crystals based upon a marcasite-like packing. *Am. Minera.* **22,** 48.

——— (1936) The symmetry and crystal structure of manganite, Mn(OH)O: *Zeit. Krist,* **95,** 163–174.

BUSER, W. AND P. GRAF (1955) Radiochemische Untersuchungen an Festkörpern III Ionen und Isotopenaustauschreaktionen an Mangandioxyden und Manganiten. *Helv. Chim. Acta* **38,** 810–830.

——— AND P. GRAF (1955) Differenzierung von Mangan (11)-Manganit und δ-MnO_2 durch Oberflächenmessung nach Brunauer-Emmet-Teller. *Helv. Chim. Acta* **38,** 830–834.

——— P. GRAF AND W. FEITKNECHT (1954) Beitrag zur Kenntnis der Mangan (11)-Manganit und des δ-MnO_2. *Helv. Chim. Acta,* **37,** 2322–2333.

——— AND A. GRÜTTER (1956) Über die Natur der Manganknollen. *Schweiz. Mineral. Petrog. Mitt.* **36,** 49–62.

COLE, W. F., A. D. WADSLEY AND A. WALKLEY (1947), An *x*-ray diffraction study of MnO_2. *Trans. Electrochem. Soc.* **92**, 1–22.

COPELAND, L. C., F. S. GRIFFITH AND C. B. SCHERTZINGER (1947) Preparation of a dry cell depolarizer by air oxidation of manganous hydroxide. *Trans. Electrochem. Soc.* **92**, 127.

DACHS, H. (1962) Determination of the hydrogen positions in manganite, MnOOH, with neutron diffraction. *Jour. Phys. Soc. Japan*, **17**, suppl. B-11, 387–9.

——— (1963) Neutronen und Röntgenuntersuchungen am Manganit, MnOOH. *Zeit. Krist.* **118**, 303–326.

DE LISLE, R. (1772) Essai de cristallographie, 8 vol., Paris. Cited in *Dana's System of Mineralogy*, 7th ed., 1944, **1**, 646.

DE SCHULTEN, A. (1887) Note sur la reproduction artificielle de la pyrochroite. *Comp. Rend.* **105**, 1265.

DROTSCHMANN, C. (1951) *Moderne Primarbatterien.* S. 10, N. Brantz ed.

——— (1960) The properties of the lower manganese oxides. *Chem. Weekblad.* **56**, 754–7.

DUBOIS, P. (1936) Contribution to the study of the oxides of manganese. *Ann. Chim.* **5**, 411–482.

FAULRING, G. M., W. K. ZWICKER and W. D. FORGENG (1960) Thermal transformation and properties of cryptomelane. *Am. Mineral.* **45**, 946–59.

FEITKNECHT, W., P. BRUNNER AND H. R. OSWALD (1962) Über den Einfluss der Feuchtigkeit auf die Oxydation von Manganhydroxid durch molekularen Sauerstoff. *Zeit. anorg. Allgemeine Chem.* **316**, 154–160.

——— AND W. MARTI 1945a Über die Oxydation von Mangan (11) Hydroxyd mit molekularem Sauerstoff. *Helv. Chim. Acta*, **28**, 129–48.

——— AND W. MARTI (1945) Über Manganite and künstlichen Braunstein. *Helv. Chim. Acta* **28**, 148–156.

——— H. R. OSWALD AND FEITKNECHT-STEINMANN (1960) Über die topochemische einphasige Reduktion von γ-MnO_2. *Helv. Chim. Acta* **43**, 1947–50.

FLEISCHER, M. W. E. RICHMOND (1943) The manganese oxide minerals, a preliminary report. *Econ. Geol.*, **38**, 269.

———, W. E. RICHMOND AND H. T. EVANS, JR. (1962) Studies of the manganese oxides V, Ramsdellite, MnO_2, and orthorhombic dimorph of pyrolusite. *Am. Mineral.* **47**, 47–58.

FOX, R. K., D. F. SWINEHART AND A. B. GARRETT (1941) Equilibria of $Mn(OH)_2$ in solutions of HCl and NaOH: *Jour. Am. Chem. Soc.* **63**, 1779.

FRONDEL, C. (1953) New manganese oxides: hydrohausmannite and woodruffite. *Am. Mineral.* **38**, 761–769.

——— U. MARVIN AND J. ITO (1960) New data on birnessite and hollandite. *Am. Mineral.* **45**, 871.

GARRELS, R. M. (1960) *Mineral Equilibria at Low Temperature and Pressure.* Harper & Brothers, New York, N. Y.

GATTOW, G. (1961) Charakterisierung der einzelnen Braunsteinarten. *Batterien,* **15**, 201–208.

——— (1961) Die chemische Analyse von natürlichen und künstlichen Braunsteinen. *Batterien*, **15**, 163–165.

——— AND O. GLEMSER (1961) Darstellung und Eigenschaften von Braunsteinen. II Die γ- und η-Gruppe der Braunsteine. *Zeit. anorg. all. Chem.* **309**, 20–36.

GLEMSER, O. (1939) A new modification of MnO_2. *Ber. deut. chem. Ges.* **72**, 1879–1881.

——— G. GATTOW AND H. MEISIEK (1961) Darstellung und Eigenschaften von Braunsteinen. I Die δ-Gruppe der Braunsteine. *Zeit. anorg. all. Chem.* **309**, 1–19.

——— AND H. MEISIEK (1957) Reine synthetische Braunsteine. *Naturwissenschaften*, **44**, 614.

GRIGORIEV, D. P. (1934) Physical studies of the manganous hydroxides, pyrochroite and bäckströmite. *Mem. Soc. Russe Mineral.* **63,** 67–80. *Chem. Abs.* **29,** 2481–5, 1935.

HAIDINGER, W. (1827) *Roy, Soc. Edinburgh, Trans* **11,** 127. *Dana's System of Mineralogy,* 1944, 7th ed., **1,** 712.

HARCOURT, G. A. (1942) Tables for the identification of ore minerals by *x*-ray powder patterns. *Am. Mineral.* **27,** 94.

HARIYA, Y. (1961) Mineralogical studies on manganese dioxide and hydroxide minerals in Hokkaido, Japan. *Jour. Fac. Sci. Hokkaido Univ.* Ser. IV, *Geol. Mineral.* **X,** (4), 641–702.

HERZ, W. (1900) Über Gleichgewichtserscheinungen zwischen Mangansalzen und Ammoniak. *Zeit. anorg. Chem.* **22,** 279.

HEWETT, D. F. AND M. FLEISCHER (1960) Deposits of the manganese oxides. *Econ. Geol.* **55,** 1–55.

HOREN, A. (1953) The manganese mineralization at the Merid Mine, Minas Gerais, Brazil. Ph.D., Thesis, Harvard Univ.

IGELSTRÖM (1864) *Ann. Phys.* **122,** 181. *Dana's System of Mineralogy,* 1947, 7th ed., **1,** 639.

JONES, L. H. P. AND A. A. MILNE (1956) Birnessite, a new manganese oxide mineral from Aberdeenshire, Scotland. *Mineral. Mag.* **31,** 283–288.

KLINGSBERG, C. (1958) the system Mn-O-OH. Ph.D. Thesis, Penn. State Univ.

——— AND R. ROY (1959) Stability and interconvertibility of phases in the system Mn-O-OH. *Am. Mineral.* **44,** 819–838.

——— AND R. ROY (1960) Solid-solid and solid-vapor reactions and a new phase in the system Mn-O. *Jour. Am. Ceram. Soc.* **43,** 620–626.

KOVALENKO, P. N. (1956) Use of the polarograph to determine the pH at which manganese hydroxide begins to precipitate, and its solubility product. *Zhur. Neorg. Khim.,* **1,** 1717–21. *Chem. Abs.* **51,** 2363e, 1957.

KRISHNAN, K. S. AND S. BANERJEE (1939) The magnetic anisotropy of manganite crystal in relation to its structure. *Trans. Faraday Soc.* **35,** 385–387.

KRULL, F. (1932) Über die Synthese und einige Eigenschaften von Polianit, Braunit und Hausmannit. *Chem. Erde,* **7,** 473–482.

LARSON, L. T. (1962) Zinc-bearing todorokite from Phillipsburg, Montana: *Am. Mineral.* **47,** 59–66.

LATIMER, W. M. (1952) *Oxidation Potentials.* Englewood Cliffs, N.J., Prentice-Hall.

LEVINSON, A. A. (1962) Birnessite from Mexico. *Am. Mineral.* **47,** 790.

MAH, A. D. (1960) Thermodynamic properties of manganese and its compounds: *U.S. Bur. Mines, Rept. Invest.* **5600.**

MAIER, C. G. (1934) Manganese, its occurrence, milling and metallurgy, part 11, ch. 5, thermodynamic properties of manganese and its metallurgically important compounds. *U.S. Bur. Mines, Inf. Circ.* **6769,** 99–163.

MCMURDIE, H. F. (1944) Microscopic and diffraction studies on dry cells and their raw materials. *Trans. Electrochem. Soc.* **86,** 313–326.

——— AND ESTHER GOLOVATO (1948) Study of the modifications of manganese dioxide. *Jour. Res. Natl. Bur. Stand.* **41,** 589.

——— B. M. SULLIVAN AND F. A. MAUER (1950) High temperature *x*-ray study of the system Fe_3O_4-Mn_3O_4. *Jour. Res. Natl. Bur. Stand.* **45,** 35.

MILLAR, R. W. (1928) The specific heats at low temperatures of manganous oxide, manganous-manganic oxide and manganese dioxide. *Jour. Am. Chem. Soc.* **50,** 1875.

MOORE, T. E., M. ELLIS AND P. W. SELWOOD (1950) Solid oxides and hydroxides of manganese. *Jour. Am. Chem. Soc.* **72,** 856–866.

Näsänen, R. (1942) Die potentiometrische Bestimmung des Löslichkeitproduktes von Manganhydroxyd. *Zeit. phys. Chem.* **191,** 54–64.

Oka, K. (1938) Studies of fundamental reactions in analytical chemistry (part 1) reactions between metal ions and NaOH: *Jour. Chem. Soc. Japan,* **59,** 971–1013.

Palache, C., H. Berman and C. Frondel (1944) *Dana's system of Mineralogy,* 7th ed., 1 New York, N.Y., John Wiley & Sons, Inc.

Perrin, D. D. (1962) The hydrolysis of manganese II ion: *Jour. Chem. Soc.* 2197–2200.

Ramdohr, P. (1956), The manganese ores. *XX Inter. Geol. Cong. Symp. Mangan.* **1,** 19–73.

Ramsdell, L. S. (1932) An *x*-ray study of psilomelane and wad. *Am. Mineral.* **27,** 143–149.

Robinson, R. A. and R. H. Stokes (1959) *Electrolyte Solutions,* 2nd ed. Butterworths Scientific Publications, London.

Rossini, F. D., D. D. Wagman, W. H. Evans, S. Levine and I. Jaffe (1950) Selected values of chemical thermodynamic properties. *N.B.S. Circ.* **500.**

Roth, W. A. (1929) Zur Thermochemie des Eisens, Mangans und Nickels. *Zeit. angew. Chem.* **42,** 981.

Sackur, O. and E. Fritzmann (1909) Die Löslichkeit des Manganhydroxyds und der Dissoziationsdruck des Mangandioxyds. *Zeit. Electrochem,* **15,** 842.

Sato, M. (1960) Oxidation of sulfide ore bodies I geochemical environments in terms of Eh and pH. *Econ. Geol.* **55,** 928–961.

Schmalz, R. F. (1959) A note of the system Fe_2O_3-H_2O. *Jour. Geophys. Res.* **64,** 575.

Schossberger, F. (1940) *X*-ray examination of natural and synthetic manganese dioxide. *Batterien,* **9,** 17–20, 33–35, 1941. *Physik. Ber.* **22,** 1340.

Shomate, C. H. (1943) Heats of formation of manganomanganic oxide and manganese dioxide. *Jour. Am. Chem. Soc.* **65,** 785–794.

Simon, A. (1937) Über das System Manganoxyd/Wasser. *Zeit. anorg. allg. Chem.* **232,** 369–381.

Sorem, R. K. and E. N. Cameron (1960) Manganese oxides and associated minerals of the Nsuta manganese deposits, Ghana, W. Africa. *Econ. Geol.* **55,** 278.

Southard, J. C. and G. E. Moore (1942) High temperature heat content of Mn_3O_4, $MnSiO_3$, and Mn_3C. *Jour. Am. Chem. Soc.* **64,** 1769–1774.

Verwey, E. J. W. and J. H. de Boer (1936) Cation arrangement in a few oxides with crystal structure of the spinel type. *Rec. Trav. Chim.* **55,** 531–540.

Wadsley, A. D. and A. Walkley (1949) Some observations on the potential of the manganese dioxide electrode. *Trans. Electrochem. Soc.* **95,** 11.

——— (1951) The structure and reactivity of the oxides of manganese. *Rev. Pure Appl. Chem.* **1,** (4), 203–213.

Watanabe, T., A. Kato and J. Ito (1960) The minerals of Noda-Tamagawa Mine, Iwate Prefecture, Japan. II Pyrochroite ore (kimiman-ko) and its origin. *Min. Jour.* **3,** 30–42.

Werner, A. G. (1789) *Bergm. Jour.* **1,** 369 *Dana's System of Mineralogy,* 7th ed., **1,** 712, 1944.

White, D. E., J. D. Hem and G. A. Waring (1963) Chemical composition of sub-surface waters. *U.S. Geol. Survey Prof. Paper* **440-F.**

Zobell, C. E. (1946) Oxidation-reduction potential of marine sediments. *Am. Assoc. Petrol. Geol,* **30,** 477–513.

Zwicker, W., G. Meijer and H. Jaffe (1962) Nsutite—a widespread manganese oxide mineral. *Am. Mineral.* **47,** 246–266.

Manuscript received, December 11, 1964; accepted for publication, May 28, 1965.